POLITECNICO DI TORINO

Master degree course in Electronic Engineering

Master Degree Thesis

Design of a wireless power transfer class-E DC-DC converter controlled by an optimal power point tracking algorithm

Supervisor

Prof. Gianluca Setti

Co-Advisors

Prof. Fabio Pareschi

Eng. Andrea Celentano

Candidate

Tommaso Oberto

ACADEMIC YEAR 2021-2022

Summary

This thesis work aims to realize a wireless power transfer class-E DC-DC converter controlled by an innovative method. The circuit is composed of a primary and a secondary side which are isolated and works like an inverter and a rectifier stage coupled by two inductor coils (i.e. two coupled coils that work as a transformer with low coupling factor k). The wireless class-E converter is usually designed for a specific load value and a specific k and only in this configuration the optimal solution is guaranteed. Furthermore, this circuit is very sensitive to variations in the load (the simplification of the time-variant electronics that must be fed by the converter) or the coupling factor (changing with distance, misalignment or medium between the coils). The idea is to implement a control algorithm capable of guaranteeing and eventually tracking the *Optimal Power Point* (OPP) for different power levels in different scenarios that arrive from variations of the load value or the distance between the primary and the secondary circuit. This new method doesn't use a feedback mechanism based on telemetry to maintain the converter at the optimal working point, but it exploits only a regulator at the secondary side (either a series or parallel). It gives the possibility to have control based only on the primary side electrical waveforms like the input voltage and the input current.

This control method requires a voltage or current limiter at the receiver side as additional hardware parts and is based on an OPP identification in the input voltage – input current characteristic when the converter is designed in the correct way. This OPP is a corner point and so a discontinuity point in the derivative. An uncontrolled regulator dissipates too much power and so is useless, using this OPP method the minimum power dissipated is guaranteed (theoretically zero). This process can be applied both to loads requiring constant voltage or constant current driving.

In the first chapter, a little introduction to how wireless power transfer systems are normally designed is proposed followed by an introduction to the tracking algorithm method.

In the second chapter, the whole theoretical analysis is covered: the design of a general wireless class E converter is analyzed and the mathematical notions are presented. Then the innovative control method is treated and explained in all its parts, pointing out the important considerations about it. Finally, some simulations are used to verify all the previous points.

In the third chapter, a real prototype is designed using *MATLAB* and *Python* scripts and, after implementing it, some laboratory tests are done to verify the correct behaviour of the converter input voltage – input current characteristic.

Finally, in the fourth chapter, a simple control tracking algorithm is described and a possible implementation is proposed. Eventually, the conclusions are drawn.

Contents

Chapter 1

Introduction

1.1   Wireless power transfer employing class E DC-DC converters

A wireless power transfer is a system that allows the transmission of power throws an air gap between two distinct circuits. In this paper, only WPT based on the inductive link is considered, for this reason, the transmission of energy happens to throw a magnetic field. Inductive links are usually designed to operate at high frequency (i.e. in the MHz range) in order to achieve the desired performance with smaller reactive components. The idea is to use a resonant circuit, in this case, a class-E converter, to model the waveforms (for example the voltage on the switch) to have a commutation when drain-source voltage on MOS is null or when there is zero-current throw it. These are also named *ZVS* (Zero Voltage Switching) or *ZCS* (Zero Current Switching). If this happens the working frequency can be higher than the normal DC-DC converter and the efficiency can increase. *ZVDS* (Zero Voltage Derivative Switching) is when voltage arrives at zero and the derivative in time is also null. If the circuit has both *ZVS* and *ZVDS* conditions true, the class-E is working at the optimal point. In another case, when it's working with only *ZVS* true is called a sub-optimal point or relaxed condition. The circuit is an isolated resonant class-E DC-DC converter characterized by a loosely-coupled transformer. The methodology is not the classic one, but a new one which allows for achieving the same performance with a significant reduction in the number of reactive components of the circuit. So there are some benefits in terms of complexity, cost and size. Very high frequency gives the possibility to adapt the techniques used to reduce the dissipation in RF amplifiers. In parallel to the load, there is a capacitor to create a filter at the output that takes only the dc value. In the figure 1.1 there is the classic class-E approach, otherwise in the figure 1.2 is shown the new one.
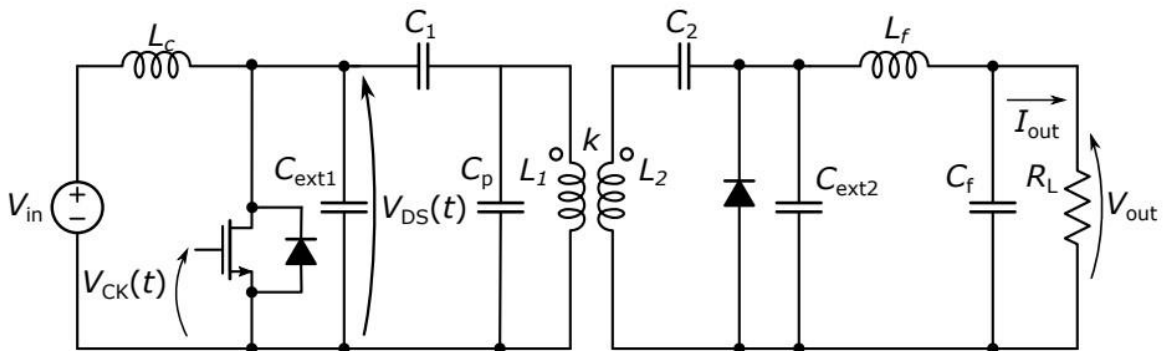
Figure 1.1 - Class-E with classical approach design
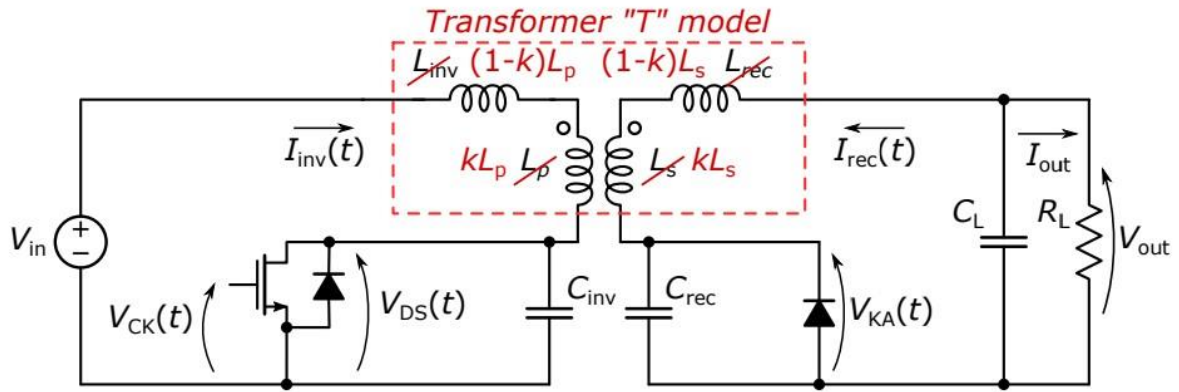
Figure 1.2 - Class E with new architecture design

The primary circuit is usually designed like an RF (Radio Frequency) power amplifier and its purpose is to drive with maximal efficiency the primary coil. The secondary circuit is designed as an energy harvesting block. In a high frequency isolated DC-DC converter the first stage is very similar to an RF amplifier acting as a dc-ac converter and the secondary stage performs like a high-efficiency rectifier ac-dc. This paper follows up on recent works in which the WPT system is designed as an isolated DC-DC converter characterized by a low coupling factor k as described in [1]-[6]. The class E converter is designed for a given operating condition, but this condition is very sensitive to variations of some parameters. Specifically, the focus is on the class E converter characterized by Zero Voltage Switching (*ZVS*) and Zero Voltage Derivative Switching (*ZVDS*). The main challenge in the design of inductive links is represented by the poor coupling between the coils and by the sensitivity of the link gain and of the received power to coil misalignment. For this reason, a WPT converter independent of variations of k, coupling factor, or load is the goal of this study.

1.2   Optimal power point identification

WPT systems are typically very sensitive to the distance between the two coils and to the load variations. When the secondary side is moved to the primary side the coupling factor k is heavily affected; an uncontrolled WPT system can guarantee the desired output power only for one specific value of the load and for one specific value of k. To solve this problem typically a feedback mechanism at the transmitter side is implemented. Information about the received power (or voltage) is sent back to the transmitter via the same link (back telemetry) as in [7] and [8]. However this solution needs more components and it's complex, the power consumption of the receiver unit increase and it drops the total efficiency.

To overcome those problems, some methods have been proposed in the Literature. They generally can be classified into primary-side control, secondary-side control and dual-side control [9]. All of these assume that the load is either a circuit that requires a constant current or a circuit that requires a constant voltage, to guarantee an output power stabilization. Some primary-side control methods can control the output power by taking into account both load and coupling factor variation. For example, [10] there is one that includes a look-up table (LUT) that implies the characterization of every link but creates a complex system. The secondary-side, described in [11] and [12], and the dual-side control methods, in [13] and [14], increase the complexity of the system and in particular of the secondary side. This is a bad feature because a small and simple circuit is always preferable and it can be adapted also in a biomedical implant. To limit this problem, inductive links that manage their operation by sensing the performance exclusively at the transmitter side are desirable. In order to control the system with k or load variations and maintain the class E in a working point that guarantees the ZVS and the nominal voltage output, the *Optimal Power Point Tracking* (OPPT) algorithm is presented.
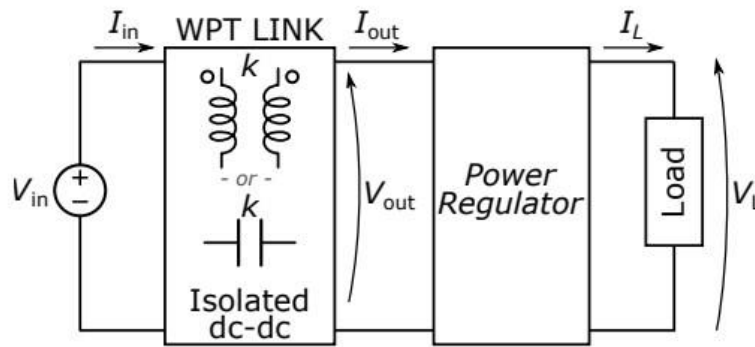
Figure 1.3 - Scheme of the circuit with the power regulator

Like in figure 1.3 a simple power regulator is added at the secondary side and, without using the telemetry, it's possible to identify the optimum working point (when the power regulator is turned on but does not dissipate any power) by simply looking at the corner point in the input voltage–input current curve characteristic in the primary circuit. This can be done without any knowledge about the value of k or about the value of the load because when the circuit is properly designed (see chapter 2.2) the optimum working point is always defined. Some works that proposed a way to face up an unknown load under a constant coupling factor or an unknown coupling factor under a constant load [11], already exist. But this OPPT method can effectively operate with both parameters being unknown at the same time and does not require any look-up tables or complex data processing.

Chapter 2

Theory

2.1 WPT class E design

The design of a class-E resonant converter is not easy due to a lot of non-linearities and reactive elements inside the circuit. For this reason, an exact symbolic solution of the circuit is not allowed, however, normally the design procedure is based on an approximated approach. The common one is the sinusoidal approximation (or first harmonic) used in RF circuits. It's divided into two steps concerning the project of the inverter stage and the rectifier. The assumption is that the input voltage of the rectifier (second stage) is a sinusoidal tone at ω_s. Normally the reflected rectifier impedance does not lead to the optimal load and so a matching network is inserted before the rectifier to ensure optimal class-E working conditions. This approach led to an only approximated solution and most important this works only if the sinusoidal assumption is true.

For this reason, a new methodology is used, state of art given by [15] and [16] Also here the converter is isolated and there is a distinction between the inverting stage and the rectifier stage, as shown in figure 1.2. The first one includes a MOS as a controlled switch, the second one includes a diode like a non-controlled switch. In this case, a semi-analytic design approach based on the system of differential equations regulating the converter evolution is proposed. This approach is dimensionless and based on the design of a normalized converter: 1 V output voltage, 1 W output power, 1 rad/s angular frequency for a fixed duty cycle D. After it's denormalized to the desired value of output voltage or output power. This approach gives the possibility to cut complex high-Q filters or matching networks and it has a good impact on the dimension and complexity of the total system. The circuit is always designed for a specific working point or operating condition, that is the one that ensures the nominal output power (or voltage). In figure 2.1 the normalized converter is shown, the real components are substituted with normalized ones (like capacitors that become $1/q_i$ or MOS that become ideal switches). The solution of the circuit lead to the definition of the four normalized state variables $i_{inv}(\theta)$, $i_{rec}(\theta)$, $v_{DS}(\theta)$ and $v_{KA}(\theta)$. They described the evolution of the circuit with normalized time θ. It's established that $\theta = 0$ is the instant of time when MOS is switched on and $\theta = 2\pi$ when MOS is switched off. All arrive from external MOS control that drives the switch with a certain commutation frequency f_s and a duty cycle D. The model is periodic with a period equal to 2π. $i_{inv}{}^{(0)}$, $i_{rec}{}^{(0)}$ and $v_{KA}{}^{(0)}$ are defined at $\theta = 0$ and the values of the state variables,

in the exact instant when the configuration of the circuit change, is used like the initial conditions for the next configurations. The evolution is taken with mathematical functions and they are used to optimize the solutions. So these functions can be used to describe the *ZVS* or *ZVDS* with mathematical notions; now using a software numerical tool, like *MATLAB*, manipulation of parameters of the circuit can be done to find an optimal configuration of class E.
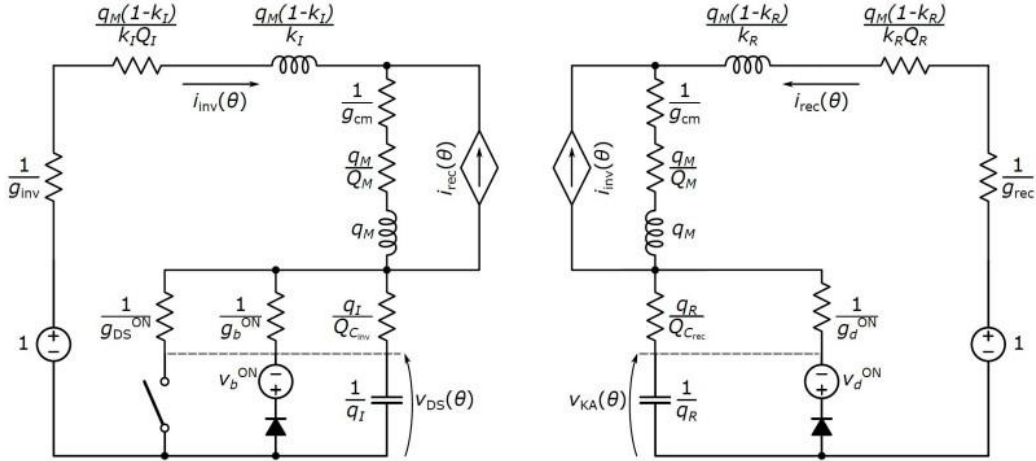
Figure 2.1 - Scheme of the normalized converter

The complete circuit can be described by five parameters:

$$q_I, q_R, q_M, k_I \text{ and } k_R.$$

Putting together, with a fixed duty cycle and project parameters ($V_{in}, V_{out}...$), there is a system of seven equations and eight unknowns (below):

$$i_{inv}^{(0)}, i_{rec}^{(0)}, v_{KA}, q_I, q_R, q_M, k_I \text{ and } k_R.$$

There are only two degrees of freedom, and after that they are taken, the solution can be found for almost all the combinations of the parameters. Using k_I and k_R like degrees of freedom is possible to have some advantages: they fixed the ratio of the inductors in the circuit. The selection of the inductors is typically the most constrained problem in circuit design. Another good feature arrives from an opportune choice of k_I and k_R, in fact $L_{inv}=0$ and $L_{rec}=0$ are possible and it simplifies the circuit. Finally, the transformer is modelled according to coupling factor k and the turns ratio n_p/n_s. Due to these equations:

$$k = \frac{M}{\sqrt{L_p L_s}} = \sqrt{k_I\, k_R} \qquad (2.1)$$

$$\frac{n_p}{n_s} = \frac{L_p}{L_s} \tag{2.2}$$

it can be defined:

$$M = k \sqrt{L_p L_s} \tag{2.3}$$

$$L_p = L_s \left(\frac{n_p}{n_s}\right)^2 \tag{2.4}$$

$$L_s = L_p \left(\frac{n_s}{n_p}\right)^2 \tag{2.5}$$

and finally:

$$k_I = \pm k \, \frac{L_p}{L_{inv} + L_p} \frac{n_s}{n_p} \frac{V_{inv}}{V_{rec}} \tag{2.6}$$

$$k_R = \pm k \, \frac{L_s}{L_{rec} + L_s} \frac{n_s}{n_p} \frac{V_{rec}}{V_{inv}} \tag{2.7}$$

k_I and k_R can be considered the extension of the coupling factor k of the transformer, a parameter quite difficult to control. Otherwise, k_I and k_R are both independent variables and also mutually bounded because $k_I \, k_R < 1$ independently of other parameters. An exhausting explanation of how the WPT link is designed can be found at [18].

The solution space can be plotted in a 2D graph, this allows to identify areas where the solutions exist and where there aren't. In figure 2.2 the solution space of a class-E converter with a $D = 50\%$ is shown. With k_I and k_R like degrees of freedom, we have some points related to optimal solutions (*ZVS* and *ZVDS*) and others to sub-optimal solutions (only *ZVS*). The yellow area represents the *ZVS* or the relaxed condition. Here there are points with low k_I and k_R values and so also k is a low value. While the blue area represents the points that guarantee a *ZVDS* condition. The red curve is the upper limit and above it there aren't space solution useful. High k values increase the possibility to have a probably *ZVDS* condition and so both current and voltage on when the MOS is switched on. But practically circuit designed on a high value of k aren't feasible and so the converter needs to work in a relaxed condition and it can manage the current at the transition.
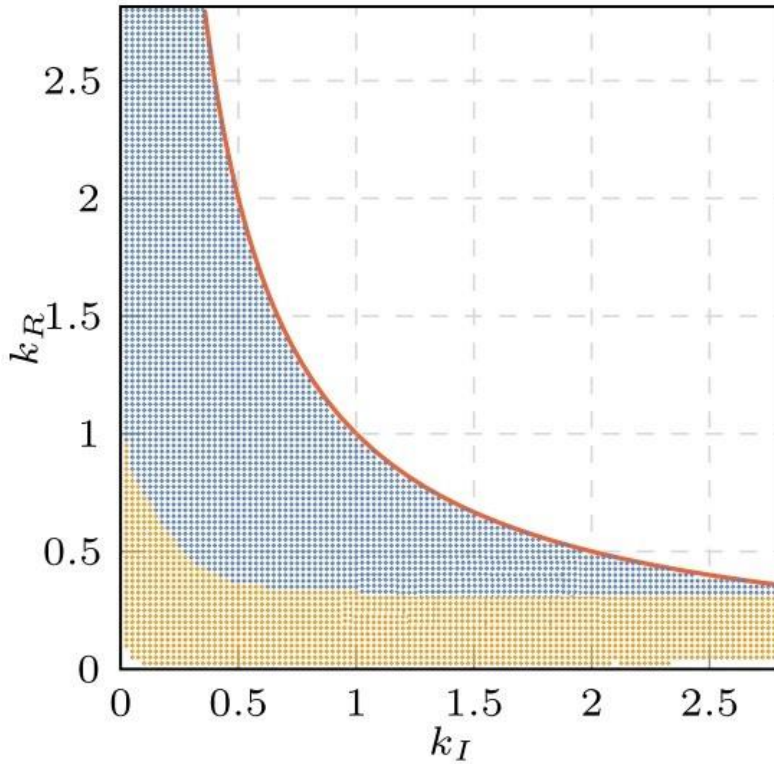
Figure 2.2 - K_I and K_R solution space

Sometimes only *ZVS* is needed, this condition relaxes the requirements for a class-E converter. A sub-optimal solution is not unique because $dv_{DS}(\theta)/d\theta$ when the MOS is turned on is not fixed to 0. Now an additional degree of freedom is introduced. Respect looking at $v_{DS}(\theta)$, the focus can be putted on $i_{inv}^{(0)}$ because if $i_{inv}^{(0)} = 0$ this leads to *ZVDS*, if not $i_{inv}^{(0)} < 0$. For a bigger value of $|i_{inv}^{(0)}|$ there will be a smaller value of q_I, q_R and q_M ; this leads to smaller inductors and bigger capacitance values. It's a huge advantage because smaller inductors are always welcome and they help to reduce the size of the converter. Otherwise, capacitors' size typically is not a problem and large values can help to compensate parasites of semiconductors. Farther for a sub-optimal solution the peak value of $v_{DS}(\theta)$ and $v_{KA}(\theta)$ is a bit less with respect the optimal case, but the *RMS* value of the currents increases and so this negatively affects the efficiency of the converter with respect to an optimal solution.

2.2   Fundamental about the optimal power point

The WPT link is modelled as an isolated DC-DC converter based on a low and unknown coupling factor k. It is schematized as a voltage controlled black box, the output power P_{out} is a monotonically increasing function of the input voltage V_{in} and of the value of k. In this section assumed that the efficiency is $\eta = 1$, so that $P_{out} = V_{out}I_{out} = V_{in}I_{in}$. The

load requires a nominal power $P_N = V_N I_N$, but this is unknown to the WPT block; the power at the load is $P_L = V_L I_L$. It's assumed that the power regulator circuit is designed on purpose to guarantee the required P_N, its behaviour is the following. If $P_{out} < P_N$, the regulator is off and does not dissipate any power. When $P_{out} > P_N$, it turns on and dissipates the excess power $P_{out} - P_N$, so that $P_L = P_N$. The optimal working point occurs when the power limiter is on, but with a negligible dissipated power, so that $P_{out} \approx P_N$.

This condition is called the *Optimum Power Point* (OPP) because, among all points that ensure the correct power to the load, this is the one requiring the minimum amount of power from the source.

P_{out} is a monotonic and invertible function of V_{in} therefore the OPP is defined for a value of V_{in} called V_{in}^{opt}. It's not an a-priori computed value because it depends on k and P_N, which are both unknown; so this new method is very interesting because the working point can be identified without those two values.

This corner point in V_{in} - I_{in} graph can be easily detectable as a discontinuity in the derivative located at $V_{in}=V_{in}^{opt}$. Two different cases with different designs with simple power regulator circuits are taken into account.

In the first case, the load is designed to work with a constant current I_N and it regulates its power by changing its voltage, so the regulator is a series regulator that limits the load current I_L into I_N. In the second case, the load is a circuit designed to work at constant voltage V_N and it regulates its power by changing its current. The regulator in this case is a shunt that limits the voltage V_L to V_N.

1 - Constant current driven load

The assumption is that load is modelled as a current-controlled circuit with actual current I_L and voltage $V_L = f(I_L)$. Nominal power is P_N and to have that load power P_L is equal to it a series current limiter is insert inside the circuit. This ensure that maximum I_L will be I_N.

The simplest implementation of the current limiter is using a BJT (or Bipolar Junction Transistor) working on its active region and biased with constant base current. In this configuration the collector and the emitter current are equal and proportional to the bias current. Figure 2.3, below, represents the theorical scheme.
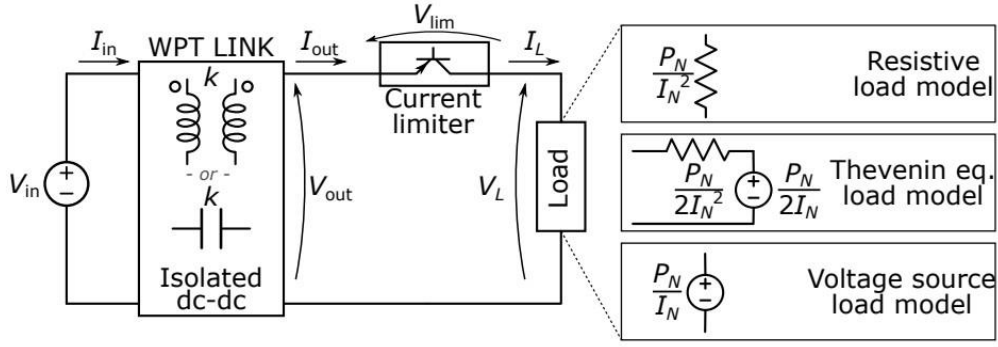
Figure 2.3 - Scheme of the constant current driven load

The OPPT works if the WPT system can be modeled as real controlled voltage source that is mathematically described as:

$$V_{out} = \alpha\, V_{in} - R_{out}\, I_{out} \tag{2.8}$$

with R_{out} small and α that depends on k (coupled factor). Now a significant distinction needs to be done: R_{load} is the ohmic value of the load, the one that is connected at the secondary side, and R_{out} (which also defines $G_{out} = 1/R_{out}$) is the output resistance of the converter with no load. R_{out} is a very sensible variable that depends on a lot of parameters like the distance of coil or current throw the circuit. So very important parameters are R_{out} which needs to be small enough (more about it in the next chapter) and k because g is directionally proportional to it. If the series regulator is assumed to be on, then $I_{out} = I_L = I_N$ and $V_L = f(I_N)$ leads to:

$$I_{in} = \frac{V_{out}\, I_{out}}{V_{in}} = \frac{(\alpha V_{in} - R_{out}\, I_N)\, I_N}{V_{in}} \approx \alpha I_N \tag{2.9}$$

this is true for $V_{in} > V_{in}^{opt}$ with:

$$V_{in}^{opt} = \frac{P_N}{\alpha I_N} + \frac{R_{out}\, I_N}{\alpha} \approx \frac{P_N}{\alpha I_N} \tag{2.10}$$

Both approximations are valid only if R_{out} is small. If the current regulator is off (no power is dissipated by it) $V_{lim} = 0$ and $V_{out} = V_L$. Now some assumptions on the $f()$ characteristic of the load is required. Three different load model are proposed: a *resistance model*, a *Thevenin equivalent model* and a *voltage generator load model*.

Resistance load model

This first model represents the load like a resistance, voltage is defined as:

$$V_L = \left(\frac{P_N}{I_N^2}\right) I_L \tag{2.11}$$

Since $I_L = I_{out}$ and putting $V_{out} = V_L$ this led to:

$$I_{out} = \frac{\alpha V_{in}}{\left(R_{out} + \frac{P_N}{I_N^2}\right)} \tag{2.12}$$

If R_{out} is smaller, the approximation of I_{in} is:

$$I_{in} \approx \frac{\alpha^2 I_N^2}{P_N} V_{in} \tag{2.13}$$

Thevenin equivalent load model

In this Thevenin equivalent circuit at nominal I_N half power is dissipated in voltage generator and other half in the resistance. So:

$$V_L = \frac{P_N}{2I_N} + \frac{P_N}{2I_N^2} I_L \tag{2.14}$$

imposing $V_{out} = V_L$ led to:

$$I_{out} = \frac{\alpha V_{in} - \frac{P_N}{2I_N}}{\left(R_{out} + \frac{P_N}{2I_N^2}\right)} \tag{2.15}$$

and if R_{out} is small enough the final approximation of the current is:

$$I_{in} \approx \frac{2 \, \alpha^2 I_N^2}{P_N} V_{in} - \alpha I_N \tag{2.16}$$

Voltage generator load model

The load is seen like a voltage load model and so:

$$V_L = \frac{P_N}{I_N} \tag{2.17}$$

The output current is:

$$I_{out} = \alpha V_{in} - \frac{P_N}{I_N} \tag{2.18}$$

and the input current, that in this case hasn't an approximation, is:

$$I_{in} = \frac{\alpha P_N}{R_{out} I_N} - \frac{P_N^2}{R_{out} I_N^2} \frac{1}{V_{in}} \qquad (2.19)$$

All three models hold for $V_{in} < V_{in}^{opt}$. Those three models are implemented on a general *Python* code (appendix A.1) and in the figure below all of them are represented. The R_{out} is bigger enough to validate the previous concepts and a corner point is created when BJT switch on itself to limit the current in the circuit. When lines are dashed the model is no more valid, the continuous line is the valid one. For each of three different models of the loads the OPP is defined. The resistive one has a lower slope and so this is the more sensible load model. The voltage generator load model has a higher slope and so it's easier to define the corner here.
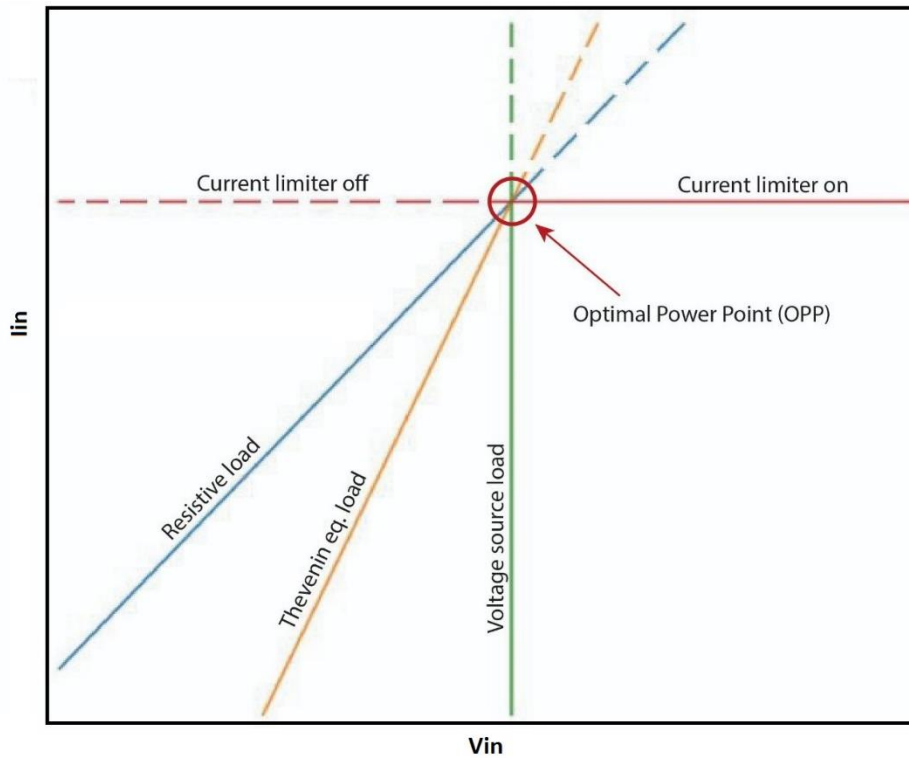
Figure 2.4 - V_{in}-I_{in} characteristic observed at the isolated DC-DC input port

2 - Constant voltage driven load

Here the load is modeled as a voltage-controlled circuit with actual voltage V_L and current $I_L = f(V_L)$ because it's a circuit designed to work at a constant nominal voltage V_N. This is the most common case and also the one used later on prototype. A parallel shunt

voltage regulator is used to limit the output voltage V_L to V_N, the simplest implementation is using a standard Zener diode like in figure 2.5.
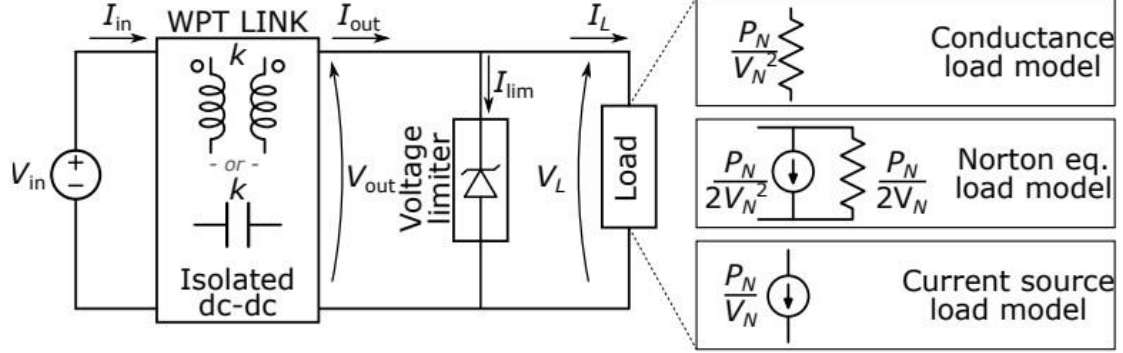
Figure 2.5 - Scheme of the constant voltage driven load

The OPPT is effective if the WPT system can be modeled as real controlled current source that is mathematically described as:

$$I_{out} = g\,V_{in} - G_{out}\,V_{out} \tag{2.20}$$

with G_{out} small and g that depend on k. Assuming that the shunt regulator is on so $V_{out} = V_L = V_N$ and $I_L = f(V_N)$ considering the formula above we have:

$$I_{in} = \frac{(gV_{in} - G_{out}\,V_N)\,V_N}{V_{in}} \approx gV_N \tag{2.21}$$

This is true for $V_{in} > V_{in}^{opt}$ with:

$$V_{in}^{opt} = \frac{P_N}{gV_N} + \frac{G_{out}\,V_N}{g} \approx \frac{P_N}{gV_N} \tag{2.22}$$

Both approximations are valid only if G_{out} is small. If the shunt regulator is off (no power is dissipated by it) $I_{lim} = 0$ and $I_{out} = I_L$. Now some assumptions on the $f()$ characteristic of the load is required. Three different load model, like in previous case, are proposed: a *conductance model*, a *Norton equivalent model* and a *current generator load model*.

***Conductance load model*:**

Here the load is seen like a conductance and so current can be defined as:

$$I_L = \left(\frac{P_N}{V_N^2}\right) V_L \tag{2.23}$$

This definition led to:

$$V_{out} = \frac{gV_{in}}{\left(G_{out} + \dfrac{P_N}{V_N^2}\right)} \tag{2.24}$$

And if G$_{out}$ is assumed small:

$$I_{in} \approx \frac{g^2 V_N^2}{P_N} V_{in} \tag{2.25}$$

Norton equivalent load model

In a Norton equivalent load model at nominal V$_N$ half of the power is dissipated in the current generator and the other half in the resistance. This led to a current:

$$I_L = \frac{P_N}{2V_N} + \frac{P_N}{2V_N^2} V_L \tag{2.26}$$

From this formula the V_{out} is:

$$V_{out} = \frac{gV_{in} - \dfrac{P_N}{2V_N}}{\left(G_{out} + \dfrac{P_N}{2V_N^2}\right)} \tag{2.27}$$

and assuming again Gout to be small:

$$I_{in} \approx \frac{2\,g^2 V_N^2}{P_N} V_{in} - gV_N \tag{2.28}$$

Current generator load model

Finally, with a current generator load model:

$$I_L = \frac{P_N}{V_N} \tag{2.29}$$

Here no approximations are possible and so:

$$I_{in} = \frac{gP_N}{G_{out}V_N} - \frac{P_N^2}{G_{out}V_N^2} \frac{1}{V_{in}} \tag{2.30}$$

All three models hold for $V_{in} < V_{in}^{opt}$, as defined in (2.22). Those three models are implemented on a general *Python* code (appendix A.1). Selecting nominal value of V_N, P_N, G_{out} and g is possible to simulate a specific load behaviour in all three models and when shunt goes on (like figure below). When lines are dashed the model is no more valid, the continuous line is the valid one.
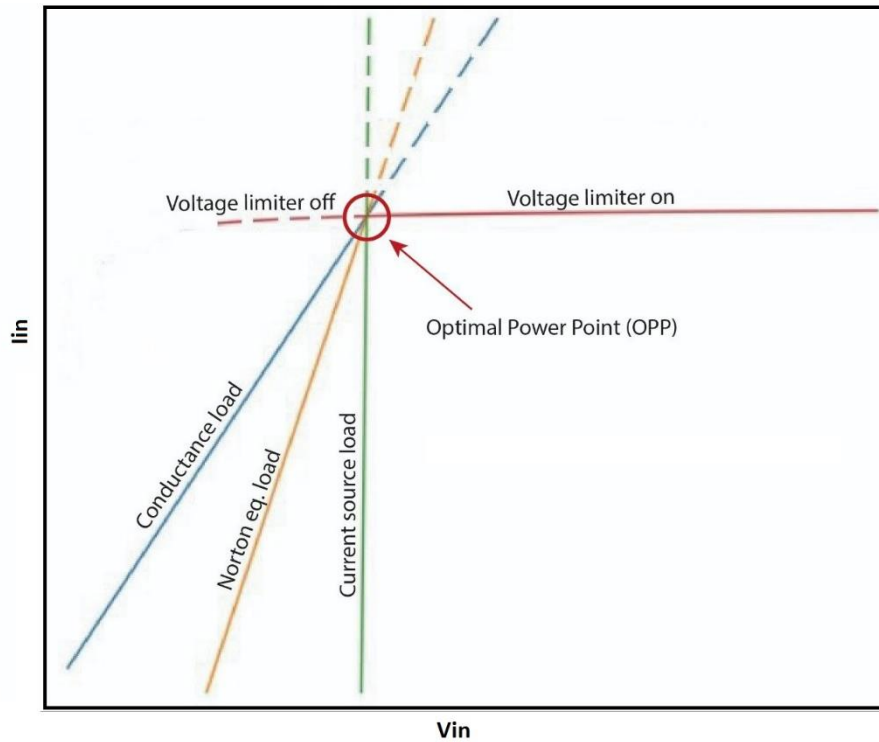
Figure 2.6 - V_{in}-I_{in} characteristic observed at the isolated DC-DC input port with high R_{out}

Here the G_{out} is small enough to verify the previously theoretical fundamentals and it can be clearly seen that the OPP is identified by the discontinuity in the derivative of V_{in} - I_{in} curve. After this point, the shunt turns on and the current on the primary side is almost constant. This working point can ensure the optimal state of the circuit and it's defined for different k and R_{load} due to G_{out} constrain that is satisfied.

Indeed the image below, figure 2.7, shows some different curves. In this case, the G_{out} is too big respect the G_{load} and so for this reason the corner point is not present. The shunt curve has a hyperbolic behaviour that creates a concavity that gives problems. In fact this is the theoretical curve, in practice this hyperbole fuses with the load model and creates a line that is not a corner and so useless for this purpose. If this happens the OPP algorithm cannot be used and it cannot discriminate the optimal working point only from the primary side. It needs information about secondary and its exit from this analysis.
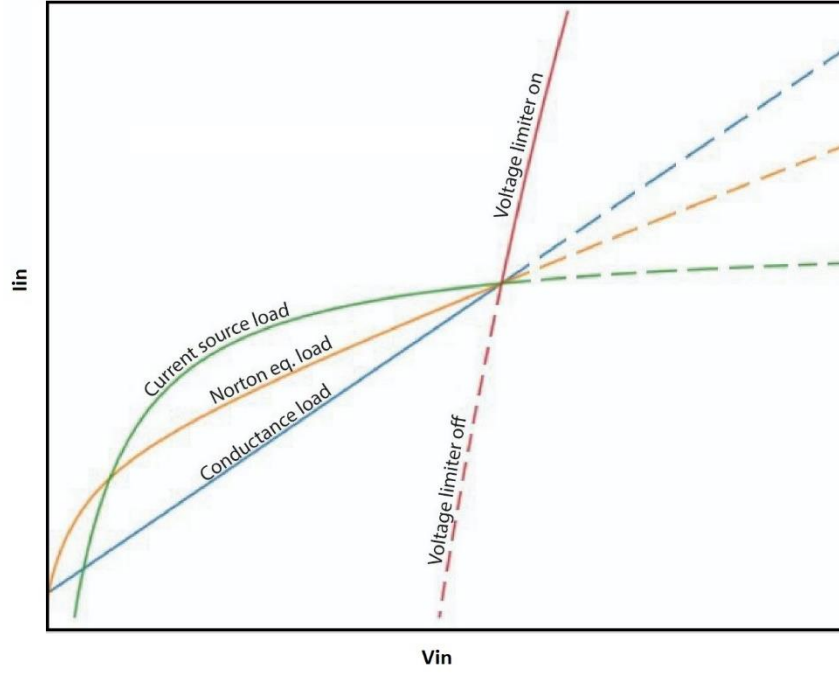
Figure 2.7 - V_{in}-I_{in} characteristic observed at the isolated DC-DC input port with low R_{out}

2.3   Important design considerations

To design a real circuit implementation some important considerations are taken into account. In the analysis above is has been assumed that efficiency is η=1. In a real circuit this behaviour is not true, but to correctly identify the OPP is enough that efficiency is almost constant or with small variations. The key point of all the design is related to a small output resistance of the converter stage in case of constant current driven load and to a small output conductance (or big output resistance) in case of constant voltage driven load. The OPP works only if a corner point in V_{in} - I_{in} curve can be easily observed. Let's put the focus on the resistance (or conductance) load model because is the load's model with a lower slope and so a lower derivative, it's the worst case to detect the corner point. Starting with the constant current driven load case the slope of the I_{in}, plot in figure 2.6, for the resistance case is constant as $\alpha^2 I_N^2/P_N$ (2.16). This value needs to be greater than the actual slope of V_{in}-I_{in} when the current limiter is on. So the derivative of (2.9) at $V_{in} = V_{in}{}^{opt}$ is $R_{out}\,\alpha^2 I_N{}^4/P_N{}^2$.

So comparing this two values, final result is:

$$R_{out} \ll \frac{P_N}{I_N^2} \tag{2.31}$$

In case of constant voltage driven load, using a similar computation, it can be shows that final result is:

$$G_{out} \ll \frac{P_N}{V_N^2}$$ (2.32)

Those results, as said before, are the keys point of the entire paper. They lead to a lot of different *MATLAB* and *SPICE* design simulations to understand how the R_{out} (and so the G_{out}) is affected by different characteristics in the circuit. The V_{in} - I_{in} curve doesn't have a well-defined corner point and the OPP cannot be identified if the R_{out} - G_{out} parameters is not sufficiently smaller with respect to the R_{load} - G_{load}. Typically results show that for a design with a very high k (something bigger than 0.5) and a properly R_{out} - G_{out} no problems arrive and normally the OPP is well defined. However it can be shown that $k = 0.5$ correspond to the distance that is between the two different sides of a PCB, so it's not realistic to design a circuit with those parameters.

For this reason, it's important to find the probable value of R_{out} for different k_i - k_r (so as different k). A lot of different *SPICE*'s simulations were made to verify and validate results with different design specifications. *SPICE* is a tool that was used a lot for made simulations, but compared to real operations it doesn't guarantee very high precise values due to some problems. Those issues probably arrive from the high residue of the *MATLAB* solution. This leads to electrical waves with a huge value with respect to their average and so their RMS values are also too high. This create some results that have a not realistic average values, but the overall behaviour gives a lot of useful information. However it help to find the total behaviour of the circuit in different situations and so it was useful to use it for this purpose.

Another parameter that changes the R_{out} of the circuit is the current at the switch-off transition of the MOS. Indeed it can be put as zero for a perfect zero voltage derivative switching mode, but in this design case the circuit is in a relaxed operative mode and so the current can be chosen like little bigger or lower than zero. It's modified in order to have a higher R_{out} as possible using different design start parameters like q_I, q_R or others.

Summing up, the converter is working at a suboptimal point (relaxed condition). There is a degree of freedom because the current inside the primary side at the commutation is not defined and so can be chosen by the designer. Trying with simulations and real circuits it has been understood that this choice gives different values of R_{out}. It's an important result because now new operating designs can be done by choosing the correct current value at the transition that gives a value of R_{out} highest as possible. One possibility is to minimize the current, another one is trying to find the value of the current at the commutation that gives the best R_{out} as possible by increasing and decreasing it.

2.4 Verification of fundamentals

To validate the analysis proposed for the OPPT approach in this section a WPT system is simulated and analyzed. The design of the circuit is made with a *MATLAB* script that gives the value of the component of the WPT starting from the initial parameters. In this section only ideal components are used for sake of simplicity. The idea is to simulate the R_{out} of the circuit and also plot the V_{in} - I_{in} curve to find the OPP. The focus is only on a WPT with a constant voltage driven load because the final prototype works like that, but the theory can be applied also at a constant current driven load like it was said before. In particular the prototype board has implemented a resistance that simulates a conductance load model and a constant current source that simulates a current generator load model (see chapter 3.1). So also the simulation takes care of those two different scenarios.

All the simulations were done in *SPICE*. The important point is to simulate a certain circuit only when it's in a stationary condition. In fact, the resonant WPT need some cycles to arrive at the final voltage on load. This is due to the capacitor that we put in parallel to R_{load}. If the capacitor is too small the stationary condition arrives earlier but the ripple at the output voltage is too big and creates problems. If the capacitor is too big, the ripple is like zero but the output voltage has a constant average value after very huge numbers of cycles. The goal is to put a capacitor that guarantees a very good ripple and to take the results of the simulation only after a lot of cycles to be sure that the values are not corrupted. The evolution of the output voltage is shown in the figure 2.8 below.
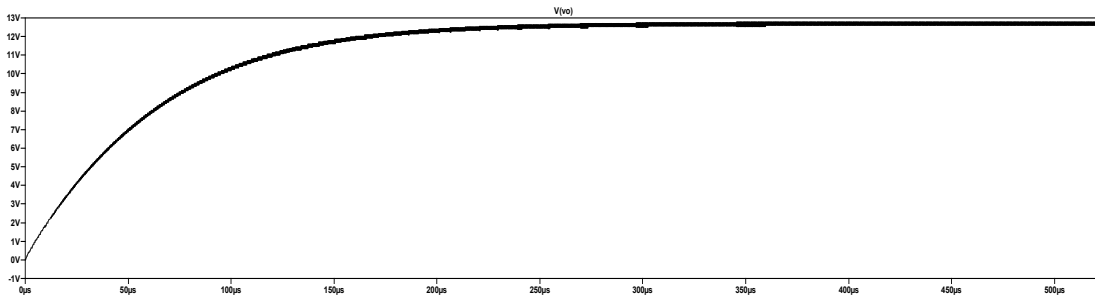
Figure 2.8 - Evolution of the output power

The schematic use for the voltage limiter in case of conductance load G_L and a voltage limiter (or shunt regulator) is shown in figure 2.9. It's based on a transconductance difference amplifier with gain g. Assuming that $G_{out} \ll G_L \ll G_I$ the open-loop gain is $A = g/G_I$ and $V_{lim} \approx A V_{ref} / (1+A)$ and this approximate V_{ref} for sufficiently large values of A. When the shunt regulator is on $V_L \approx V_{ref}$ and when $V_L < V_{ref}$ the diode is turned off and so the limiter doesn't work. The work of C_I is to limit the bandwidth because it adds a pole at $f = g/(2 \pi C_I)$ approximately. For this section, A is set to $A=100$ and limits the bandwidth to 1/10 of the switching frequency.
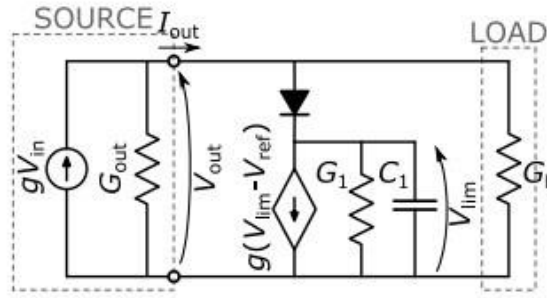
Figure 2.9 - Scheme that simulate the voltage limiter

This design uses a classic 'T' model for the isolation of the transformer that gives a coupling factor k and a total inductance L_p and L_s for the primary and secondary coil respectively. From previous formulas, the transformer can be described by the mutual inductance $M = k\sqrt{L_p L_s}$ and by the two leakage inductances $(1 - k)L_s$ and $(1 - k)L_p$ which aren't negligible due to the low value of k. The transformer is the only magnetic element required because those two inductances are used to set the resonant frequency at the primary and the secondary side.

The specifications for this design are: f_s = 6.78 MHz, output power is $P_{out,nominal}$ = 67 mW with an output voltage of $V_{out,nominal}$ = 13V and it's achieved for $V_{in,nominal}$ = 3.88 V and $R_{load,nominal}$ = 2.52 kΩ. $L_p = L_s$ = 1.87 µH and $k_{nominal}$ = 0.163. So due to this k arrive: $M_{nominal}$ = 307nH. Like degree of freedom k_R = 0.55 is chosen and this leads to k_I = 0.049. As is said before the MOS and the diode are modelled like ideal devices with a 0.7 V of voltage drop for the rectifier diode and for the MOS body diode. Inductors have been considered with Q = 110 (quality factor) and the capacitors with very high Q and so taken like ideals. The MOS is driven with a D = 0.5. The values of the capacitors given by the *MATLAB* code are C_{rec}= *290* pF and C_{inv}= 161 pF. The solution of the four state variables $i_{inv}(\theta)$, $i_{rec}(\theta)$, $v_{DS}(\theta)$ and $v_{KA}(\theta)$, that arrive from *MATLAB*, is shown in the figure 2.10.
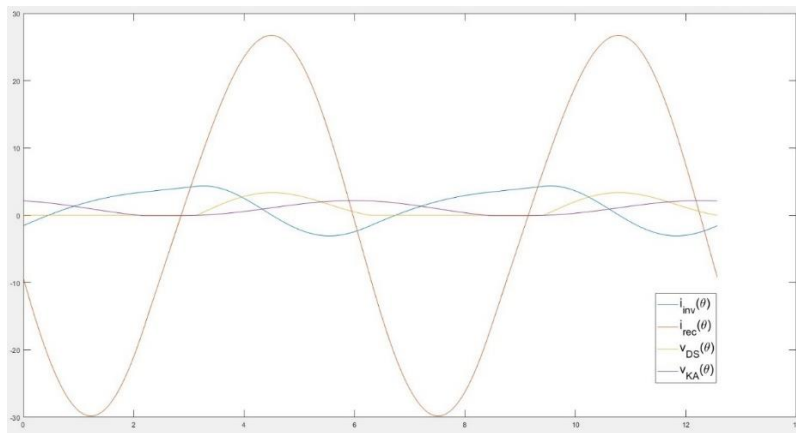
Figure 2.10 - Solution of the four state variables that arrives from MATLAB

For first, the *MATLAB* solution needs to be tested in a *SPICE* environment to understand if the circuital solution is working in the right way. The output voltage (so the power) need to be the nominal one when $R_{load} = R_{load,nominal}$, $M = M_{nominal}$ and $V_{in} = V_{in,nominal}$. Another constraint is that the circuit needs to work at least in *ZVS* (Zero Voltage Switching) condition. This is mandatory because the goal is to work in a working point that guarantees good efficiency and optimal working point of the class-E converter and this is possible only if the MOS is switched on only when the $v_{DS} = 0$ at that instant. If the *MATLAB* circuit result has these requirements it can be used for simulations.

Two different *SPICE* circuits are used for two different purposes. The first goal is to estimate the $R_{out} (= 1/G_{out})$ of the secondary circuit. For doing that the shunt is not inserted in the scheme and the converter is a class-E wireless power transfer designed with this new approach. The figure 2.11 shows the complete scheme with a capacitor of 40 nF in parallel to the load.
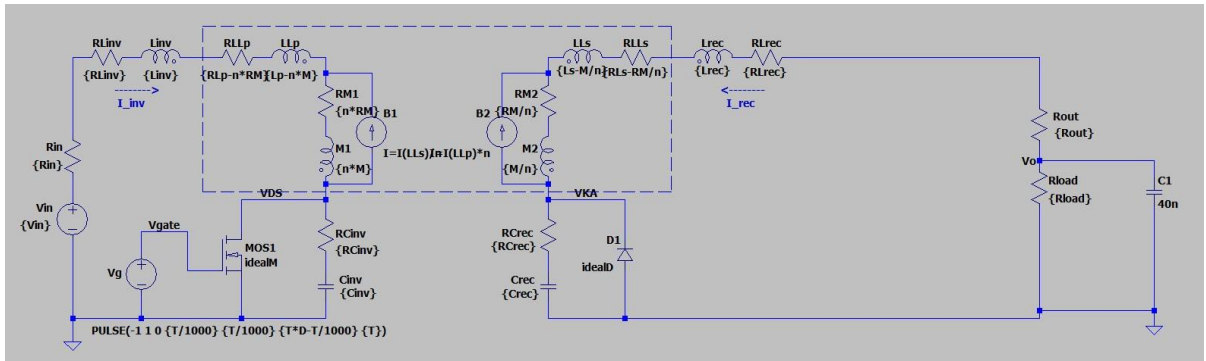
Figure 2.11 - Scheme used in SPICE of the converter without the regulator

In the first simulation the R_{load} varies in a given range and the V_{in} is maintained fixed. This allow to have different V_{out} and I_{out} that are used to estimate the R_{out}. R_{out}, therefore G_{out}, is calculated in this way:

$$R_{out} = \frac{dV_{out}}{dI_{out}} = \left| \frac{V_2 - V_1}{I_2 - I_1} \right| \tag{2.33}$$

$$G_{out} = \frac{dI_{out}}{dV_{out}} = \left| \frac{I_2 - I_1}{V_2 - V_1} \right| \tag{2.34}$$

Of course the value is not very precise, but the idea is to have an estimation of it because the theory needs only that G_{out} need to be smaller (like one order of magnitude) respect the G_{load} or R_{out} bigger than R_{load}. The value of the R_{load} for have $P_{out} = 67$ mW and so $V_{out} = 13$ V is:

$$R_{load,nominal} = \frac{V_{out,nominal}^2}{P_{out,nominal}} = \frac{36\,V^2}{67\,mW} = 2522\,k\Omega$$

The simulation starts from $R_{load} = 1$ kΩ and arrives at $R_{load} = 4$ kΩ with a step of 100Ω; for two different value of $V_{in} = 2.9$ V and 3.9 V (nominal one). The mutual inductance M, which has the same meaning of k and so it varies when the two inductances are moved away from each other, doesn't change in this simulation and its $M_{nominal} = 307$ nH. To analyze the data exported from the simulation, a *Python* code tool is used to process and plot the results. The I_{out} - V_{out} characteristic is plotted below (in figure 2.12) for the two different values of V_{in}. The current source behaviour of the load here becomes clear.
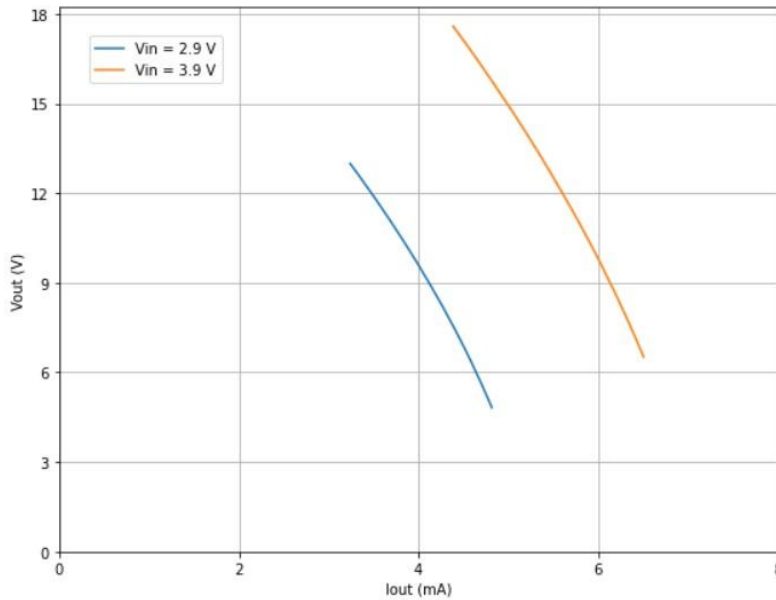
Figure 2.12 - I_{out}-V_{out} characteristic of the simulated circuit

The estimated G_{out} is plotted in figure 2.13. It's clear that the G_{out} is lower than $G_{load,nominal} = \frac{P_{out,nominal}}{V_{out,nominal}^2}$ (like 4-5 times) in both cases, this provides the constraint that is needed to have a visible OPP, like shows in theory. Also here the curves are plotted for two different V_{in} because data are taken from the same simulation. The very important result is in an interval near the $V_{out,nominal} = 13$ V because it's the nominal value of V_{out}.

The blue curve represents the G_{out} simulated with a fixed $V_{in}=$ 2.9 V then the orange curve with a fixed $V_{in}=$ 3.9 V. The green curve is the representation of the $G_{load,nominal}$ and it's needed to compare them with respect to the G_{out} when a different input voltage is applied.
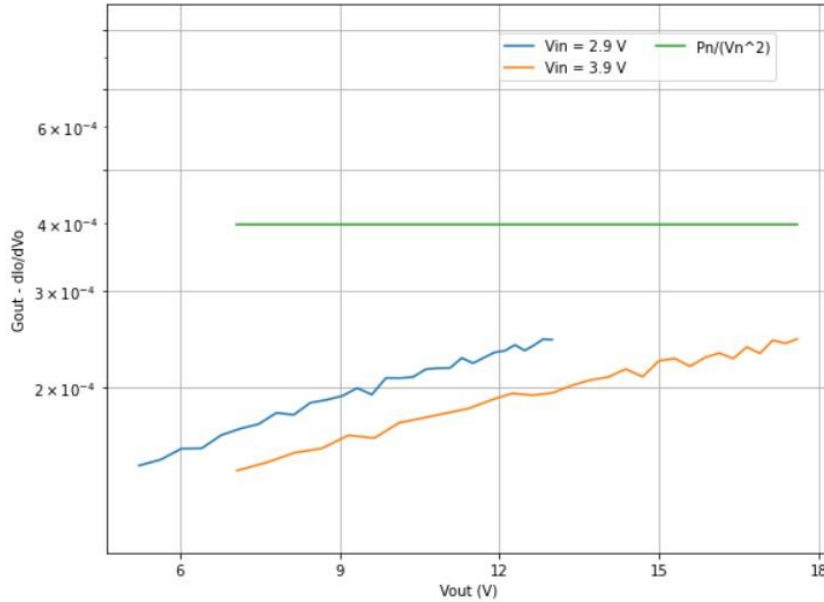
Figure 2.134 - G_{out} characteristic of the simulated circuit

The second goal is to implement the OPP and so this *SPICE* circuit implement also the shunt regulator. This shunt is modelled like showing before and it's switched on only when $V_{out}=$ 13 V and then it maintains that value. In the figure the circuit is shown, also here the capacitor has a value or 40 nF and the simulation is taken only after a lot of cycles to be sure that the circuit is in a stationary condition.
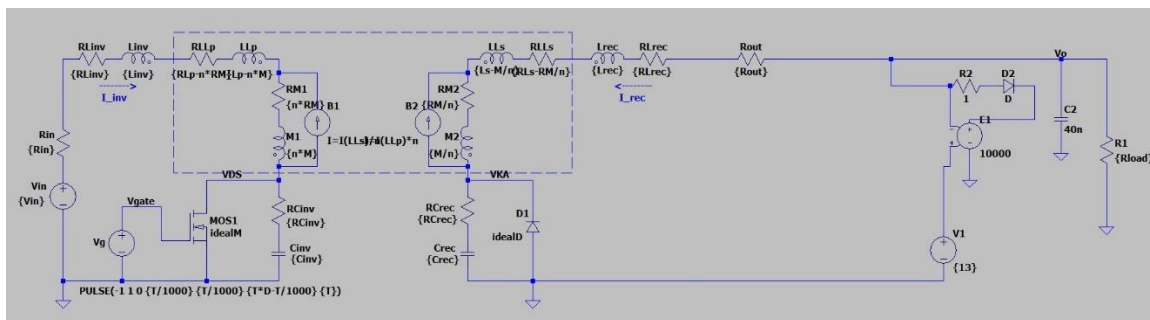
Figure 2.14 - Scheme used in SPICE of the converter with the regulator

In this case, the idea is to set a given R_{load}, that fixed a certain P_{out}, and then vary V_{in} to take the I_{in} and plot the final graph. This is done for three different values of $M = 307$ nH (nominal), 220 nH and 380 nH and also for two different values of $R_{load} = 2.52$ kΩ (nominal) and 2.167 kΩ that gives two different values of $P_{out} = 67$ mW and 78 mW respectively. In the second P_{out} case, the circuit is also simulated with a current generator with $I_{out} = 6$ mA to test the different current generator load models and to guarantee $P_{out} = 78$ mW. The V_{in} varies from $V_{in} = 1$ V to $V_{in} = 8$ V with a step of 200 mV. A *Python* code is used to manage the data, interpolate and process the final curves visible in the figures below.
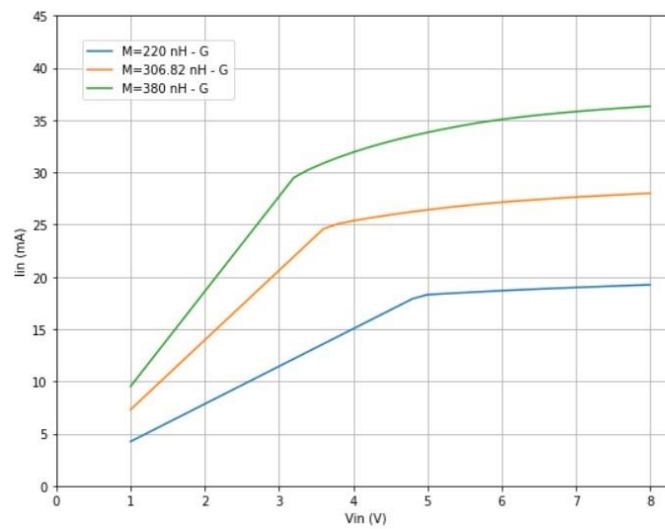
Figure 2.15 - V_{in}-I_{in} characteristic for constant power $P_{out} = 67$ mW
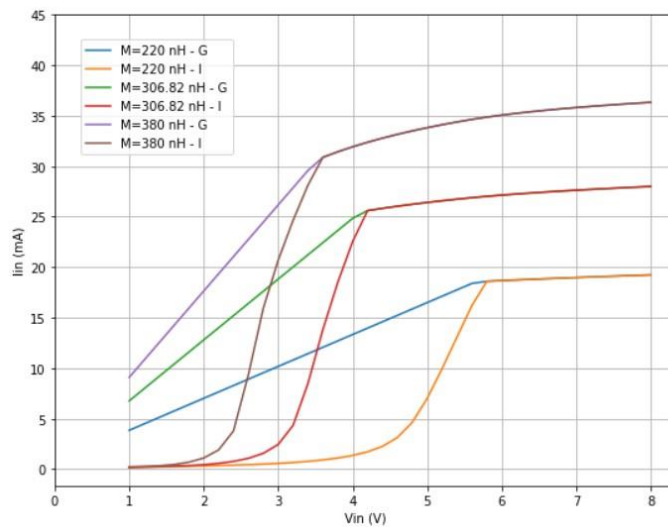
Figure 2.16 - V_{in}-I_{in} characteristic for constant power $P_{out} = 78$ mW

28

A higher value of mutual inductance M is when the two inductors (or the two parts of the converter) are closer with respect to a lower value of M. Increasing M the value of V_{in} that is needed to work in the corner decrease, but the current increase. The results of those simulations, which use circuits with ideal switches, validate the previous theory assumptions. In the first figure 2.15 there is only the conductance load model at P_{out} = $P_{out,nominal}$ = 67 mW and in the second figure 2.16 both conductance and current generator load model are used at P_{out} = 78 mW. Where the curve becomes flat is due to the voltage limiter that fixed the output. In each curve there is always present a clear point where the different slope creates a huge discontinuity in the derivative. This point with the given V_{in} and with the right value of R_{load} can guarantee $V_{out,nominal}$ = 13 V using the minimum dissipation as possible and maintain the class-E in the optimal working point. This is the *Optimal Power Point* and it can easily define by looking only at the primary current and voltage if the circuit is working in this way. When the load is modelled as a current source generator the OPP is more visible because the slope of the load has a higher slope and creates a lower angle of the corner. This behaviour is only possible thanks to the higher value of R_{out} respect R_{load}, like it's shown in the simulation before.

Chapter 3

Prototype

3.1 Project specifications

Now that the theory is verified, the idea is to design a general class-E WPT converter that can be controlled by an *Optimal Power Point Tracking* algorithm in a real environment with lossy elements. To do that first all the specifications design needs to be selected. The choice of those is related to an earlier project of a wireless power transfer converter that was implemented in the laboratory, but it can't be used for the purpose proposed in this section. In fact, its R_{out} is too small with respect to its R_{load} and so the OPPT cannot be applied because the corner inside the V_{in} - I_{in} graph doesn't exist. So the focus is to start from this implemented board and to modify it to control the converter with this new method. The amazing point is that with this design architecture, maintaining the same nominal parameters with respect to the previous project, another design needs to be done but practically there is only to change the capacitors values and the nominal load value to respect the old implementation. The capacitors are the ones that control the trend of the voltages and currents throw both primary and secondary circuit and so changing those also the R_{out} change. A lot of different implementations are designed using the *MATLAB* code and the results are simulated to understand if the converter can be controlled in this way. The key to the design is to understand that the current at the time instant zero, so $i_{inv}^{(0)}$, can be used as another degree of freedom and that it can be modified to give the results that are searched. Therefore the current is not zero when $v_{DS} = 0$, but it has a negative value and due to this the circuit works in a relaxed condition, also called *ZVS*. The R_{out} can be modified by deciding the value of this current at the transition and so the OPPT control can be applied.

The first specification that is chosen is the k, in fact, the one used for the prototype is the same that is used in the previous chapter and so $k_{nominal} = 0.163$. One constraint is related to the coils. They are difficult to realize and more difficult to characterize, so the choice is related to the only pairs available and completely characterized in the *LAB* and so they are taken from the previous board. The two coils are identical on the primary and at the secondary side with $L_S = L_P = 1.47 \ \mu H$ and a quality factor of $Q = 55$ at the central frequency of 6.78 MHz. Thanks to this k and those values of inductances the mutual inductance is $M = 240$ nH . Using this k and after a lot of trials, the initial values used in the *MATLAB* code are:

$$k_I = 0.1, \quad k_R = 0.275, \quad q_I = 0.4251, \quad q_R = 0.1001,$$

$$q_M = 0.0266, \quad i_{inv}^0 = -4.9604 \ mA, \ i_{rec}^0 = 1.3051 \ mA, \ v_{ka}^0 = 2.289 \ \text{mV}$$

The specifications are the following one: the voltage output is selected to be $V_{out,nominal}$ = 6 V. The power is therefore $P_{out,nominal}$ = 57.6 mW with a $V_{in,nominal}$ = 3,625 V and $R_{load,nominal}$ = 625 Ω. This range of voltage is important because the v_{DS} on the MOS is typically like 3-4 times bigger with respect to the V_{in} voltage and due to this the $V_{in,nominal}$ cannot be too high or a MOS with a very high drain-source max voltage is needed, with a drawback of a higher cost and a bigger area.

The central frequency is 6.78 MHz, so the circuit is designed to work in the ISM (Industrial, Scientific and Medical) band. This is a very high frequency respect classical DC-DC converter (typically some hundreds of kHz) and it carry a lot of advantages like a faster response and better efficiency. However, it also has some disadvantages, one of that is related to parasitic components inside a real transistor or diode that need to be taken into account before simulate a real circuit behaviour. The duty cycle of the MOSFET is selected to D = 0.5. All capacitors are ceramic ones because their quality factor is higher, Q = 10000 is chosen. An important thing is that the quality factor of the inductor typically changes with frequency, otherwise the Q related to capacitors can be considered constant.

The values of the capacitors given by the *MATLAB* solution are those:

$$C_{inv} = 239{,}65 \ pF \quad \text{and} \quad C_{rec} = 389{,}53 \ pF$$

Below is the solution of the four state variables $i_{inv}(\theta)$, $i_{rec}(\theta)$, $v_{DS}(\theta)$ and $v_{KA}(\theta)$, that arrive from *MATLAB,* in the figure 3.1. It can be shown that the current $i_{inv}^{(0)}$ isn't zero when v_{DS} = 0, it's negative and this proves that the circuit is working in relaxed condition with the $i_{inv}^{(0)}$ fixed in the code. After that the solution is given by the *MATLAB* code, it has been proved that the circuit works with design parameters like expected and in *ZVS* conditions before starting with simulations with it.

 As said before, *SPICE* simulations are used only to show the total behaviour of the circuit because they are less precise and with lower accuracy with respect to simulation done in a real environment with the prototype and the laboratory's instruments. And then also due to some convergence problems (see chapter 2.3) that create misalignments and mistakes with real world values. In fact when it has been understood that the circuit solution will work it has been implemented on the prototype and tested as well.
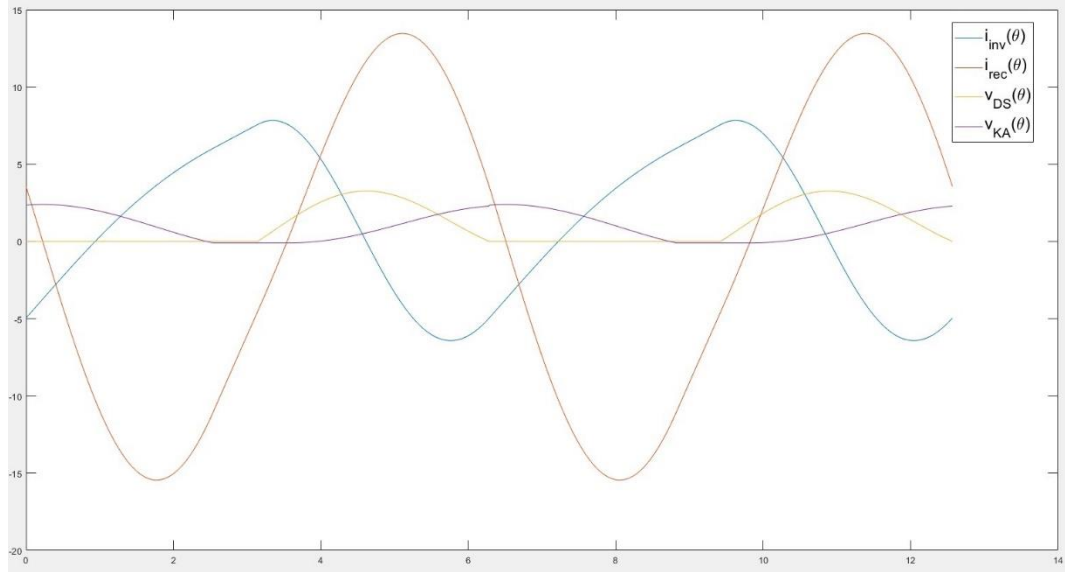
Figure 3.1 - Solution of the four state variables that arrives from MATLAB

3.2 Simulations

Like in the previous chapter, the simulations were done in *SPICE*. Also here the goal is to find an approximation of the R_{out} and to implement the V_{in} - I_{in} curve to find if the OPP is present. The first tests were done on the converter with ideal components on it. Then to have a better idea of the behaviour of the circuit, before implementing it physically, the simulations were done on a circuit that implements real models for the MOSFET and the diode. The shunt used in these simulations is modelled in the same way as before. Due to this purpose, the choice of the components is needed. MOSFET needs to have a lower $R_{DS,on}$ as possible and a $v_{DS,max}$ higher than the max peak reached by the v_{DS} voltage. The $v_{DS,max}$ that is reached depend on the V_{in}, in fact, the v_{DS} is like 4-5 times bigger than it. The chosen devices are the following:

$$Transistor\ n-MOS \longrightarrow Infineon\ IRLML0030TRPBF$$

$$Diode \longrightarrow SD103AW$$

The MOSFET has a $R_{DS,on}$ = 40 mΩ and a $v_{DS,max}$ = 30 V. So thanks to this value the max V_{in} that can be managed without problems is V_{in} = 7 - 8 V; a higher V_{in} can damage the components. The diode forward voltage of the MOS is $V_{b,ON}$ = 1 V and the diode forward voltage of the diode is $V_{d,ON}$ = 0.6 V. The real components have parasites capacitors implemented inside them, due to this the values of C_{inv} and C_{rec} need to be reduced by a factor. The datasheet of the devices says the values of those parasites' capacitors but only at 1 MHz, so to find the right value that needs to be subtracted it needs to see the v_{DS} shape. In fact, changing the capacitor values give the possibility to have the *ZVS* or not.

Choosing a final good value of C_{inv} and C_{rec} is important to have an easier implementation so:

$$C_{inv} = 239{,}65 - 139.65 = 100 \; pF \quad \text{and} \quad C_{rec} = 389{,}53 - 39.53 = 350 \; pF$$

Two different circuits are implemented to satisfy both different goals. The results using real components models are really similar to the ones that arrives from simulations with ideal components. Thanks to this, here it only showed the final results that arrive from real device simulations. Below in the figure 3.2 and 3.3, there are the two *SPICE* circuits used to simulate the controller. The C_{out} used is 200 nF because it's a good value in this case to decrease the output voltage ripple and to give steady-state measurements in a useful time.
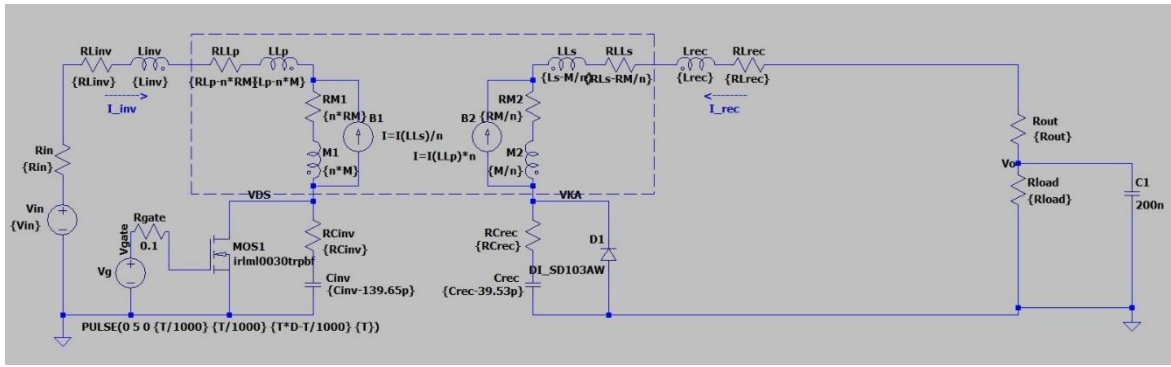
Figure 3.2 - Scheme used in SPICE of the prototype without the regulator
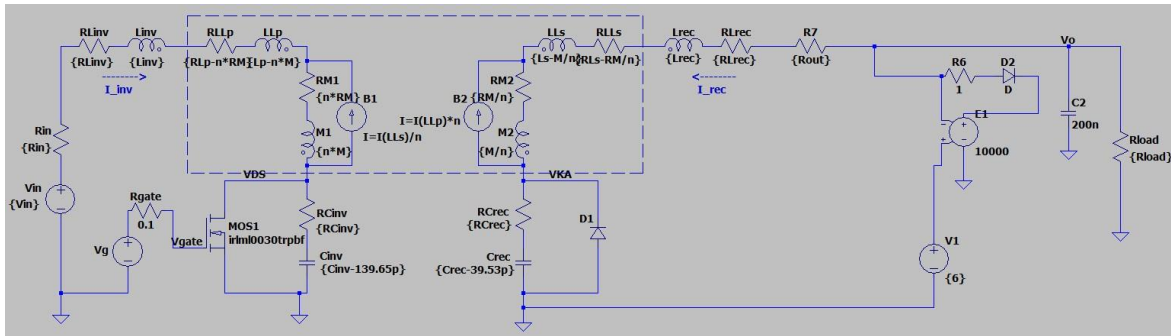
Figure 3.3 - Scheme used in SPICE of the prototype with the regulator

The two simulations done with those circuits are the following:

1) Evaluation of R_{out}: the V_{in} is setting a nominal value and the R_{load} vary. In this case, the V_{in} used is 5.5 V which is higher than $V_{in,nominal} = 3{,}625$ V like it's written in the

project specifications due to the *SPICE* values issue as explained in the chapter before. The R_{load} start from 562.5 Ω to 687.5 Ω with a step of 12.5 Ω. The *M* is fixed at the nominal one.

2) Implementation of the OPP: the R_{load} is fixed and the V_{in} varies. The circuit is the second one, in figure 3.3, and it has the regulator implemented. The V_{in} starts from 2 V and arrives at 9 V, with a step of 0.5 V to having a good resolution. The *M* is fixed at the nominal one. The results are plotted for three different values of R_{load} = 470 Ω, 625 Ω and 780 Ω.

The final results validate the theory. The R_{out} is very high with respect to the R_{load}, like one order of magnitude, in each point near the $R_{load,nominal}$ (625 Ω). Due to this, the OPP is present in the second figure, for each curve. Working at that point guarantees that the converter will work at the optimal point. This is an important result because those simulations use real components and from them, it can be understood that the OPP is feasible and it can work also in the real world. No more simulations were done on those circuits because those were implemented on a real device to be tested as well in the real environment.
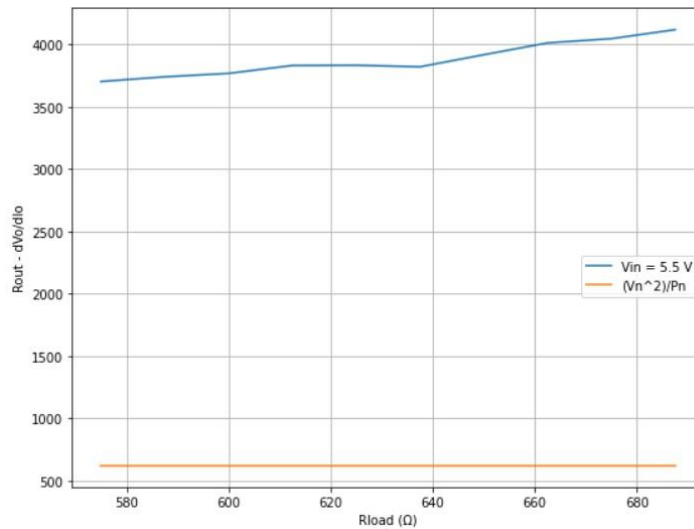
Figure 3.4 - R_{out} characteristic of the simulated prototype
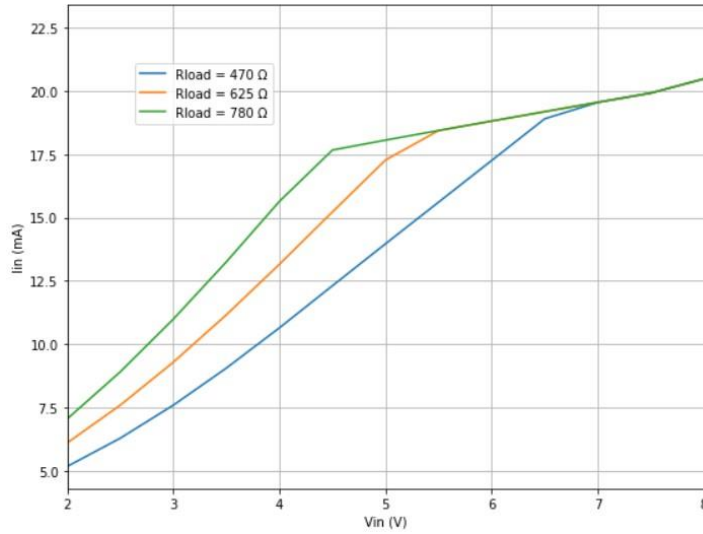
Figure 3.5 - V$_{in}$-I$_{in}$ characteristic for different power and constant M

3.3 Experimentation at nominal conditions

A WPT DC-DC converter class-E was already implemented in *LAB*, as said before. Starting from the design described in the previous chapter, this old circuit is modified to work as expected. Practically the two capacitors are changed and the load is adapted. Some shunt resistors are used to measure the current throw the primary side. The shunt regulator is inserted to work like the limiter. It's needed to maintain constant voltage when is switched on and it's implemented to have a V_{limit} = 6 V, the chosen one is:

$$Voltage\ reference \longrightarrow LT1431$$

The circuit is a DC-DC voltage converter and so it needs only a constant Vin at the input and a square wave at the gate driver to commutate the MOS. This allows having a constant V_{out}. The square wave that drives the MOS is at f_s = 6.78 MHz with a duty cycle D = 0.5, as said before. A function generator is used to create the square wave and a voltage generator for the constant voltage at the input. An electronic oscilloscope is used to see the waves inside the circuit. To guarantee that the distance between the two coils doesn't change when a constant one is needed, a sort of plastic support is used. It has some empty spaces inside that give the possibility to increase or reduce distance only increasing or decreasing the number of empty spaces between the two inductors. All the laboratory instruments can be controlled by the computer throw a general *Python* code. Using it all the parameters can be changed and modified as it wants and this simplifies and improve the probability of a better tested result. Before testing the OPP, the circuit is tested in nominal conditions to understand if the parameters are satisfied. Here below, in figure 3.6, there is the circuit powered and with the load connected. On the left, there

is the primary side with the two connectors related to the two generators. On the right, at the secondary side, only a probe is connected to see the output voltage value. The wires that go up from the board and turn around themselves are used to ease the action of the probe. On the secondary there are also other elements like a LED or some components, which arrive from the previously circuit's project and are disabled for those experiments. In this specific figure, three empty spaces are left between the two coils.
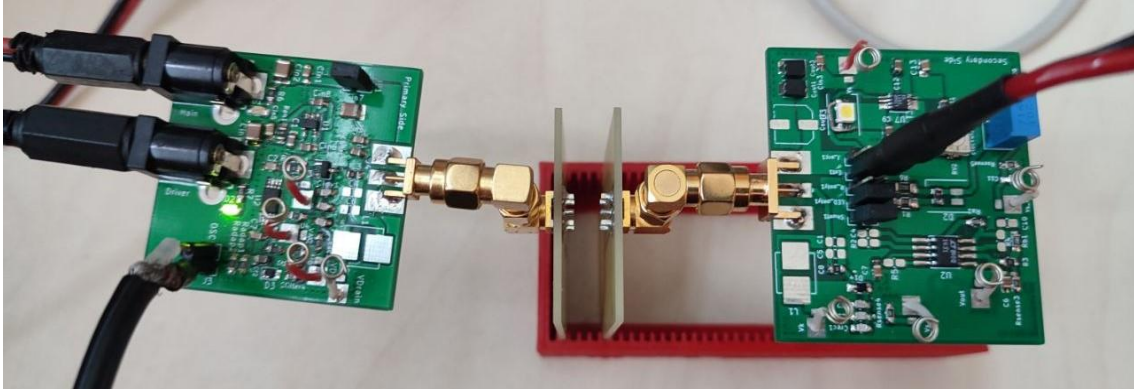
Figure 3.6 - Photo of the prototype connected and switched on

Regarding the set-up of measures, a power supply is used to correctly feed the device, so as to set the needed V_{in} at the primary side, and also to read the value of the primary current I_{in}. This is important because the *Python* code, that control also the power supply, can take this current as feedback information for the next step in the OPP algorithm. A functions generator is used to create the square wave connected to the gate-driver that switches on and off the MOSFET. The output current and voltage are measured by an active load instrument connected to the secondary side.

The nominal *M* is difficult to practically estimate, but using the other nominal parameters and moving the circuit changing the empty spaces between the two inductors is easy to find. In fact, if $V_{in} = 3.68$ V ($V_{in,nominal} = 3.625$ V) and $R_{load} = 630$ Ω ($R_{load,nominal} = 625$ Ω) to guarantee an output that is similar as possible at $V_{out,nominal} = 6$ V, three empty spaces between the two plates are used and therefore the output voltage is $V_{out} = 5.87$ V. This is the nominal operating point that works as expected. In fact, in the figures below all the important currents and voltages are shown. The circuit is working with a *ZVS* (or relaxed) condition and this ensures the right behaviour of the converter.

The first two figures show the currents in the converter. In the first one, figure 3.7, there is the i_{inv}, which is the primary current that flows inside the primary, in yellow compared with the voltage at the output of the gate driven in purple. The current has a noise curve due to the switching action of the MOS. In fact, the spikes on the current are exactly when the MOS is switched to be on or off. In the second figure 3.8, the i_{rec}, that is the current inside the diode in the secondary stage, is in yellow also here compared to

the same voltage as before. Here the noise is very low due to the isolation between the two-stage and due to the diode that is passively driven.

Figure 3.7 – I$_{inv}$-time characteristic of the prototype at nominal operation
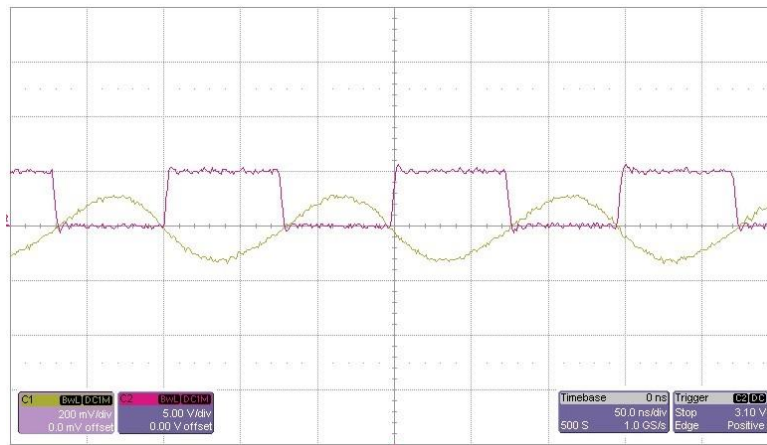
Figure 3.8 – I$_{rec}$-time characteristic of the prototype at nominal operation

The third image, figure 3.9, is probably the most important because represents the v_{DS} compared to the gate voltage, in purple. When the gate voltage has the rising edge the v_{DS} is zero or a little lower value and so this ensures that the converter is working with *ZVS*. Adjusting the values of the capacitors the transition can happen closely at possible at the zero value. In the final figure 3.10, the v_{KA}, the voltage above the diode, is shown in purple and compared with the v_{DS} in yellow. The v_{DS} cannot be too high because can damage the MOS, the maximum possible is $v_{DS,max}$ = 30 V. Due to this the Vin applied at the input of the primary side cannot be too high because the v_{DS} is normally 4-5 times bigger than it. Here in the figures, the peak of the v_{DS} is like 15 V so this is allowed and doesn't create a problem on the MOSFET. Also, the diode has a maximum peak of v_{KA} admitted that is 40 V and so also here there aren't issues in this case, but it can create

problems at higher V_{in}. Due to this reason, the maximum input voltage applied during the following test is 7.8 V.

Figure 3.9 – V_{DS}-time characteristic of the prototype at nominal operation
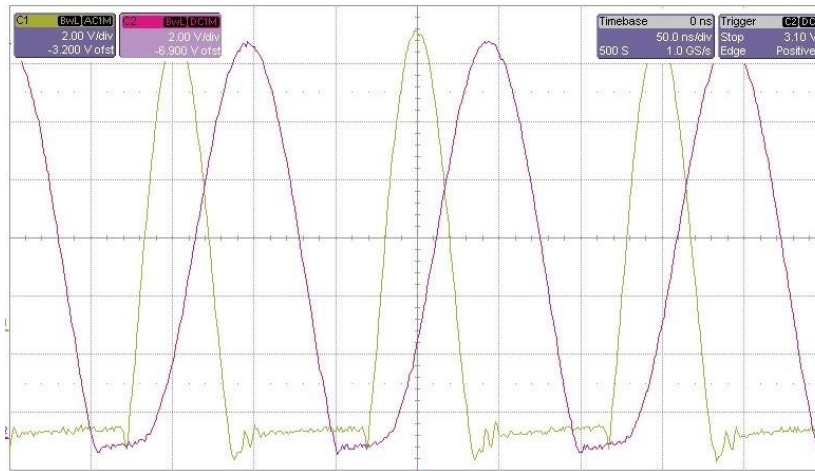
Figure 3.10 – V_{KA}-time characteristic of the prototype at nominal operation

3.3   Measurements of the optimal power point

Now that the nominal working point is checked, the OPP need to be tested. Two load models are tested: the conductance load model using a resistor like a load and the current source model using a current generator like a load. To practically implement the resistance a potentiometer is added at the output with constant resistance in series to modify the value when needed. To implement the current generator load model an integrated circuit connected to the board is used. For first the circuit is connected with a constant resistance at the load and the V_{in} is modified. Starting from 0 V up to 7.8 V with a step of 200 mV the V_{in} is increased and the respective I_{in} is saved. The R_{out} is expected

to be high respecting the R_{load} with a value near the nominal one ($R_{load,nominal}$ = 625 Ω). If this happens the *Optimal Power Point* can be easily identified like a corner in the V_{in} - I_{in} graph for different R_{load} and different distances between the two coils.

The figure below 3.11 shows the results of the test using the real prototype. The OPP is searched for three different values of distances using two, three or four empty spaces between the two coils and using five different values of R_{load} near its nominal value: 490 Ω, 560 Ω, 630 Ω (like nominal one), 690 Ω and 760 Ω. All the V_{in} - I_{in} curves show a defined corner. This is the *Optimal Power Point* and a converter with those characteristics, by looking only at this graph related to the primary side of the circuit, can be easily controlled. With the same distance, a higher resistance creates a better-identified corner with respect to a lower resistance due to a higher slope of the first section of the curve.
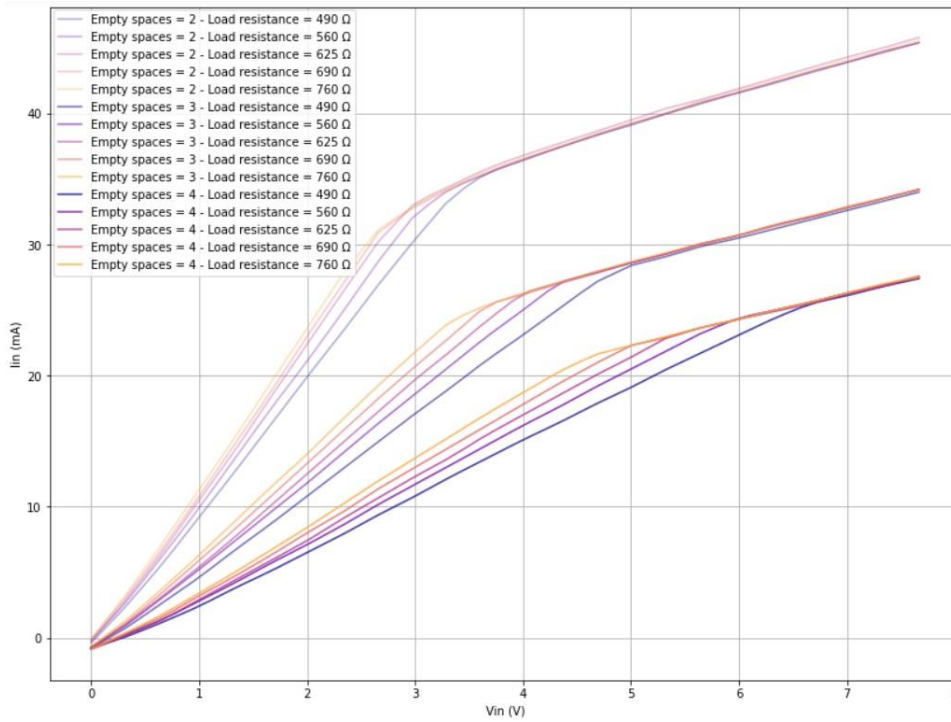
Figure 3.11 - V_{in}-I_{in} characteristic for different power and different k of the prototype – conductance load model

Then in the figure below 3.12, the OPP is searched for three different values of distances using two, three or four empty spaces between the two coils and using three different values of the current generator output near its nominal value: 7.9 mA, 10 mA, and 12.2 mA. 10 mA is the nominal one in fact 6 V * 10 mA = 60 mW that is very similar to the $P_{out,nominal}$ = 57.6 mW. Also here all the V_{in} - I_{in} curves show the *Optimal Power Point*. Here the behaviour is different because starting from the left a linear curve can be seen, this is because the generator needs a certain voltage to be completely on and then

the slope rapidly increases when the current generator is on. With the same distance, a lower current value creates a better-identified corner with respect to a higher current value due to a higher slope of the first section of the curve.
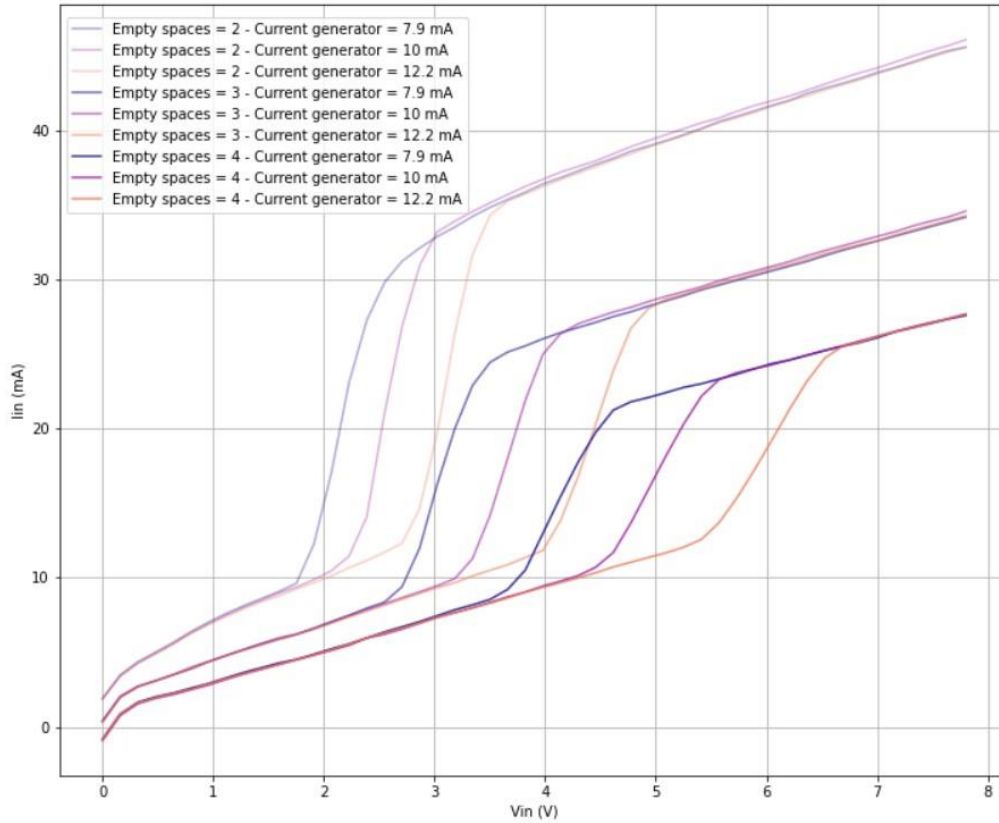
Figure 3.12 - V$_{in}$-I$_{in}$ characteristic for different power and different k of the prototype – current source load model

So both models of loads confirm that the OPP can be defined only by looking at the V_{in} - I_{in} graph at the primary side on the converter. Now the goal is to study and describe an algorithm that can control the circuit and that drives it to the optimal working point independently of load or distance variations. This is done in the following chapter.

Chapter 4

Control algorithm

4.1 Description

Now that the converter has the expected behaviour a control algorithm can be implemented. Now, in all of this chapter, the previously converter behaviour is taken for granted. This control can work only if the class-E WPT has this V_{in} - I_{in} characteristic with those corners for different parameters. The idea is to use software to work always at the optimal working point. So the algorithm needs to identify the point at the initial conditions and then understand when the parameters, like R_{load} or the distance between the two coils, change and then it needs to track back to the optimal point.

The software was written in *Python* code because using it also gives the possibility to control all the laboratory instruments at the same time. But this control can be applied, for example, by using a microcontroller and connecting it with the converter. In fact, the needed parameters that the controller needs to manage are: V_{in} which is a constant voltage at the input of the converter, one square wave voltage to drive the MOSFET with fixed frequency and duty cycle and one input to read the input current value I_{in}. No other greatness is useful to this control method and of course, this is a point of merit of this process that needs to be taken into account.

The controller doesn't know the a priori specified behaviour of the converter, so it's not an open loop control that exactly knows which V_{in} needs to be fixed to work in the chosen point. In fact the intent is to drive every circuit with this specific behaviour and not only this single prototype, the constraint is that the WPT need to be designed to have a V_{in} - I_{in} characteristic like the prototype. Due to this, the control is based only on changing the V_{in} and seeing the respective I_{in}. Starting from this and saving the behaviour of the I_{in}, a corner can be identified and the V_{in} of the converter can be fixed to work at the optimal point for a fixed R_{load} and k (related to the distance).

The goal of this chapter is to propose an algorithm that can track the optimal working point of this class-E DC-DC converter with this specific behaviour. So there aren't constrain to have a faster control as possible or the most efficient one, but to prove that using this topology control based on information that arrives only from the primary side can be done.

4.2 Proposed algorithm

In this section of the paper, a general algorithm is proposed to control the converter. Of course, a lot of different tracking algorithms can be found in the Literature, normally related to power control of the solar panels. Due to this specific and particular case, a general tracking algorithm cannot be reused in this case and so a new one is studied and proposed. This implementation is only a demonstration of how a converter can be controlled using this methodology, but there can be a lot of different practical realizations.

The algorithm needs to be a continuous loop that constantly works to find the correct point. The tracking algorithm is composed of two parts, one to define the corner point and one to understand when the steady state conditions are varying and so, when this happens, to re-start the identification and track the point. The basic idea, shown in figure 4.1, is to divide the control flow into some steps:

1. *Identification*: starting from a steady state condition with a fixed R_{load} and fixed distance (k) the algorithm needs to be able to identify the corner only by modifying the V_{in} and analyzing the respective I_{in}. Then when it finds the optimal point, it needs to fix the V_{in} so the converter is working in the correct way. The identification is used every time that a variation is found and so the optimal working point needs to be fixed again.

2. *Control of input power*: by looking at the input power, the controller can understand if the parameters of the controller, R_{load} and k, are changing. To be precisely doing this it's able to understand if the k is increasing or decreasing or if the R_{load} is decreasing and so understand where the new V_{in} optimal point will be. The control of the current is very easy and fast and so can be done a lot of times without creating problems. When the controller understands that something is changing it needs to restart the identification and find the new optimal point.

3. *Swing the V_{in}*: the V_{in} is oscillated to understand when the R_{load} is increasing. In this case, the power at the input doesn't change because the current I_{in} remains constant. The oscillation allows understanding if the corner point is always centred or not. This is done only sometimes respecting the control of the current like it's explained in the next pages. Also here when it understands that something is changing with respect to the previously steady-state conditions, it needs to restart the identification and find the new optimal point.
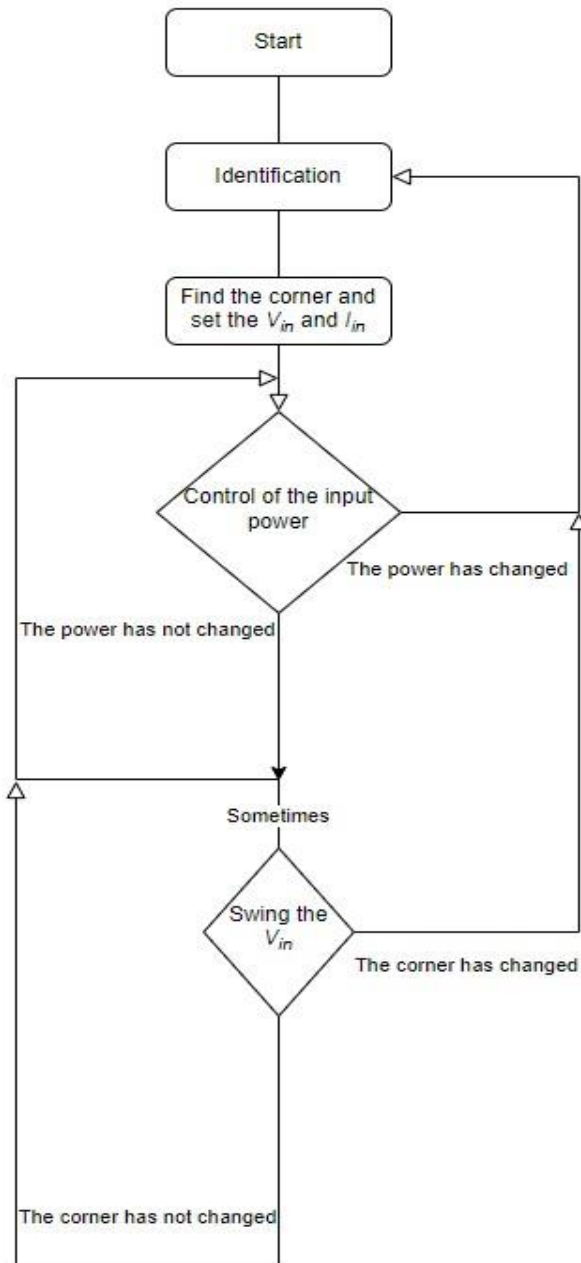
Figure 4.1 – Flow chart of controller behaviour

Identification

The identification works as it follows. Idea is to start from the highest V_{in} that is used, in the previous case 7.8 V, and go down with a given step. The step chosen in this example is 200mV. For each step, the corresponding I_{in} is taken and saved. So after that, the first three points are taken a regression straight line is created between them. The slope and the intercept of this line are saved in a *Python* vector and then another point is added, the first point is deleted and the new one is used, with the previous two, to generate a new

regression straight line. Therefore using a mobile window, that needs only three points to work, a straight line can be generated using the newly added point and two points taken at the previous steps; their parameters (slope and intercept) are saved to be compared.

The first idea to find the optimal point is to compare the slope of different lines between them. However, a simulation shows that the slope is more sensible to some noise that can arrive in a real environment and so the corner cannot be found with high accuracy. Due to this reason, the intercepts of the straight lines are used. Comparing those, starting from higher input voltages and going down, there is the possibility to practically see when this value is drastically changing for different lines. When this happens, the curve has a big mutation and this can be associated with the corner or the optimal point of the V_{in} - I_{in} characteristic.

To verify that the intercept is the key point of the identification a simulation was done. The data used are extrapolated from the real prototype behaviour and they are written in an *Excel* file. A *Python* code (appendix A2) is created to show different intercept behaviours for different R_{load} or k. So the code works as explained above, but it plots all the different intercepts that arrive from different regression straight lines for each different working condition.

The V_{in} is set in proximity of the corner point when a difference among intercept values is found, (the chosen step selects the resolution of the chosen V_{in}) so the optimal working condition of the converter is guaranteed.

In case the identification is reused, after that controller understands by monitoring the power or using the oscillations process that something is changing with respect to the previous working state, it needs to work also by increasing the V_{in} in case the expected new working value is at a higher value than before.

In the figure below 4.2, the simulation is done with the data extrapolated from the prototype with the conductance load model and so a resistance load. Here three different values of k are used (associated with different numbers of empty spaces) and three different values of R_{load} near its nominal value: 490 Ω, 625 Ω (nominal one) and 760 Ω. The red points are the values associated with every single intercept of the regression straight line generated on three different points based on a mobile window. Of course, starting from the highest value of V_{in} (at the right) and going down.

Looking from right to left, a falling curve can be detected. There is where the optimum working point is, in fact, the values of the intercepts start to decrease due to the corner. In this case, using this step value ,for example, every time that a new intercept value of a regression straight line is lower than two times a previous value the corner can be identified.
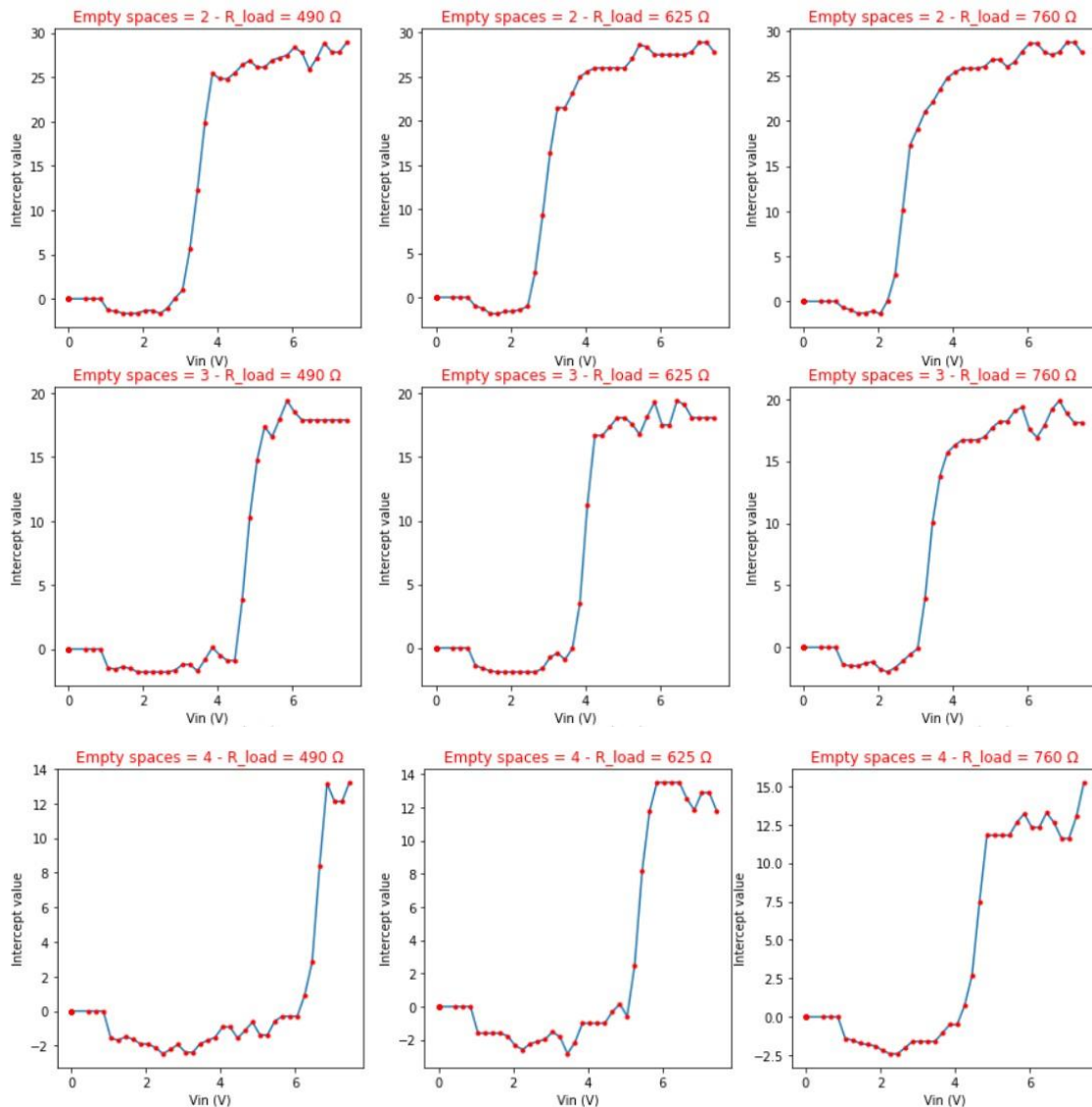
Figure 4.2 – Intercepts value with conductance load model

Matching the chosen point with the previous figure 3.11 gives the possibility to understand that the mechanism is correct. So the algorithm is able to identify this discontinuity in the derivative, in all these different situations, only by looking at this parameter.

This simulation is also tested using a current source load model and so a current source is implemented like a load. In the figure below 4.3, the results show some little variations with respect previous one. Looking from right to left, also here the V_{in} starts from maximum value and decreases, the points inside the falling slope select the corner optimum point. Then there is a rising slope that is related to the fact that the input current curve, shown in figure 3.12, of this model becomes more flattened due to the current source that needs to switch on itself.
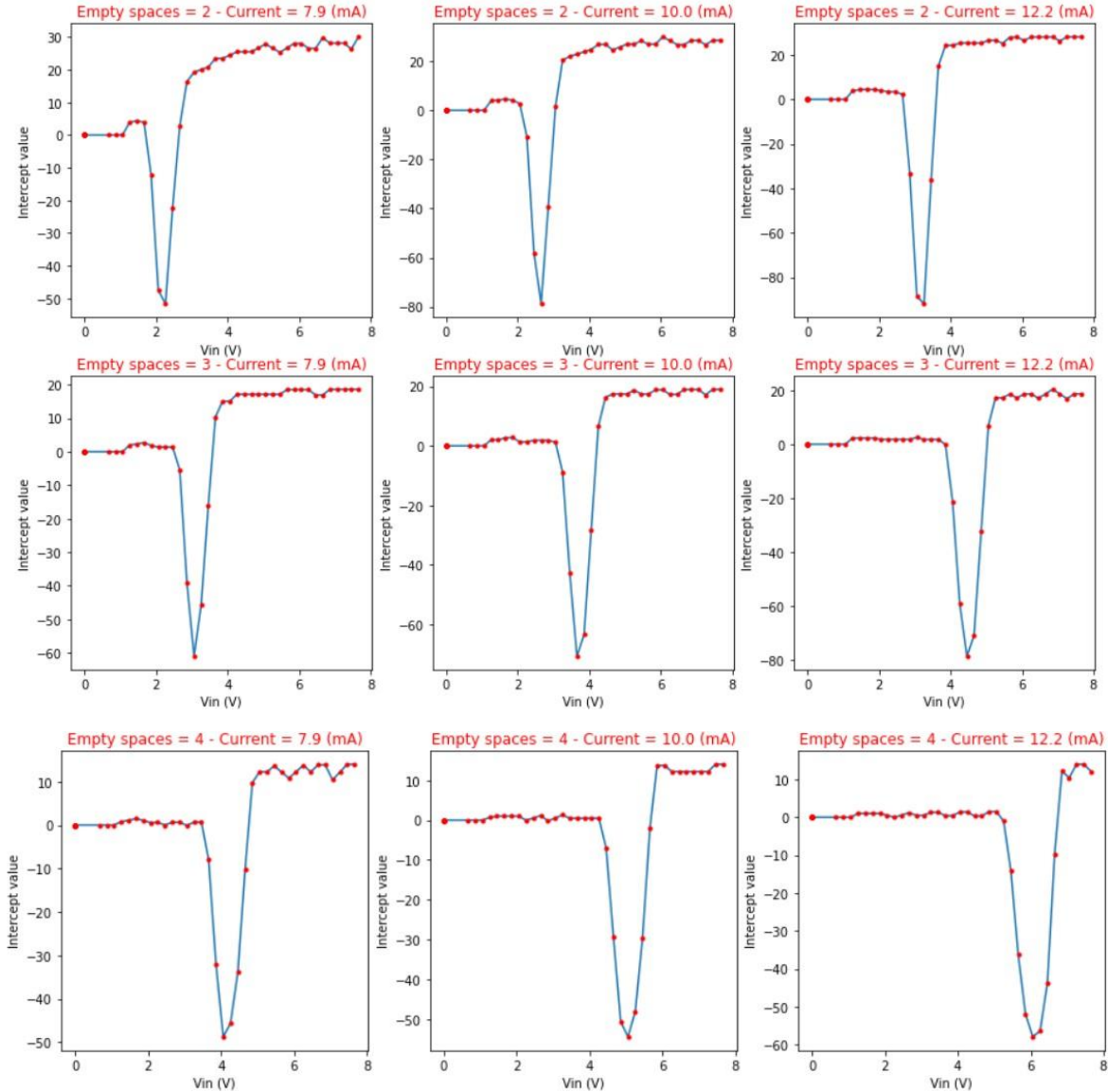
Figure 4.5 - Intercepts value with current source model

Control of input power

To understand when the converter's steady state is changing due to some variations in the distance between the two coils or to load variations, the input power can be monitored. The V_{in} is set and so by looking at the input current I_{in} the power can be always estimated. When this value has a substantial variation, the V_{in} - I_{in} curve is changing and the optimal point is no more in the working condition of the converter, a new identification needs to be done.

In a real environment with no restriction, a variation of k is more incisive in the V_{in} - I_{in} curve change with respect to a variety of load value. When this two happen together, normally the overall behaviour is more affected by the first one; however, the intensity of the two different variations needs to be taken into account to have a better estimation.

The input power changes and can be monitored only for these three different situations:

1. The distance between the two coils increases and so the k decreases → the power decreases because the input current for a fixed V_{in} decreases

2. The distance between the two coils decreases and so the k increases → the power increases because the input current for a fixed V_{in} increases

3. The load value decreases → the power decreases because the input current for a fixed V_{in} decreases

These a priori consequences are valid for all the converters that present the behaviour given by a high R_{out}. So by looking only at the trend of the power the next state of the converter can be guessed. The figures 4.4 and 4.5, below, show the two different scenarios when the k is varied. In the first one, the k is decreased and so the input power also decreases. So when the converter is working in the optimal power point and an increase of the distance between the two coils happens, the controller can understand it by only looking at the input current. If the power decreases, it knows that the new optimal power point will be at a lower V_{in} respect to the previous one used. For the same reason, when the k is increased the new V_{in} of the optimal power point will be higher than the previous one. When the controller knows that, it can restart the identification process by increasing or decreasing the V_{in} and it can use the intercepts method to find the new optimal working point.
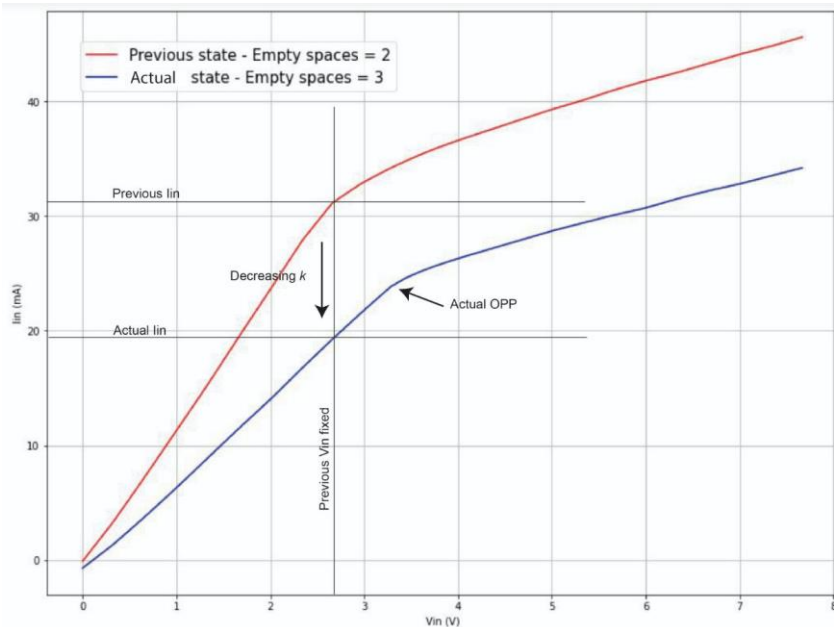
Figure 4.4 – Working point variation: k decrease
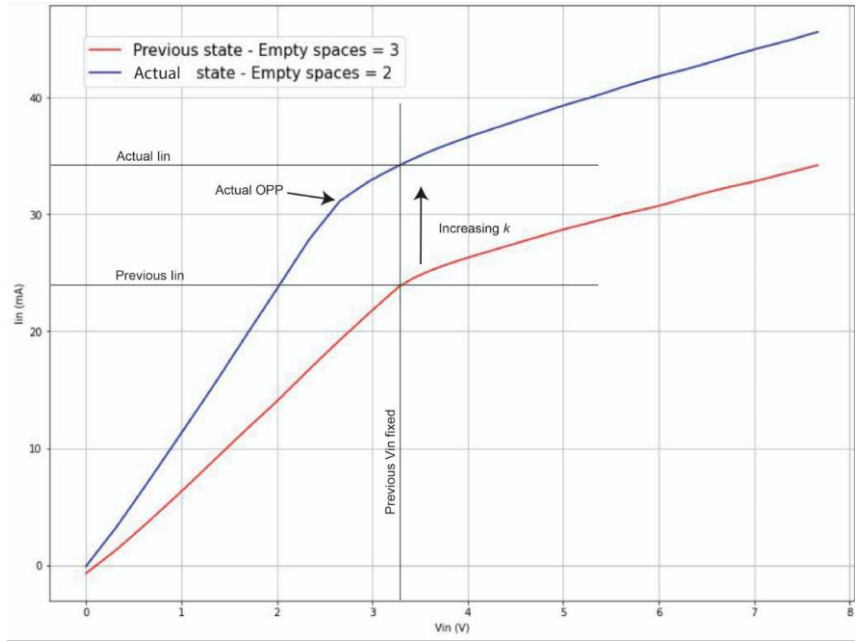
Figure 4.5 - Working point variation: k increase

It's possible to understand when the value of R_{load} decreases, and where the new optimal V_{in} will be in the next state, by only looking at the input current. Like shown in figure 4.6, the current state has a current for the fixed V_{in} that is lower with respect to the previous current value. The controller knows that the current optimal V_{in} is at a higher value than previously fixed one.
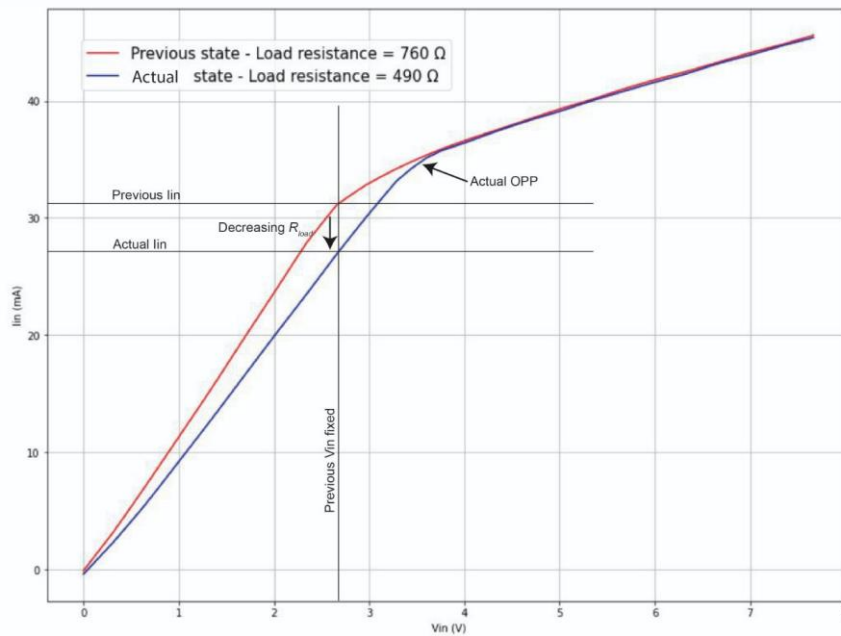
Figure 4.6 - Working point variation: R_{load} decrease

Swing the V_{in}

The fsinal case is when the R_{load} increases with respect previous value. In fact in this case the power, and so the input current doesn't change. Like shown in figure 4.7, when the R_{load} varies and becomes new higher value than previously one, the current doesn't have a variation. For this reason, the controller can't control all the variations by only looking at the input power, but it needs also to use another method to find if the controller is working in the right place.
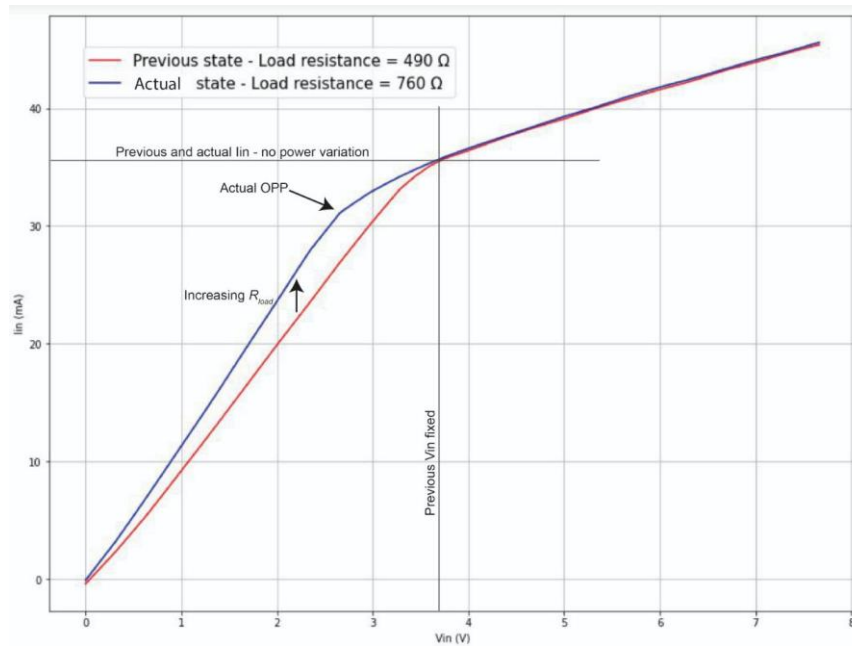
Figure 4.7 - Working point variation: R_{load} increase

The controller can swing the V_{in} to understand if the corner of the curve is always at the same point or not. Starting from the fixed V_{in} and using a selected step (from the identification part), it applies $V_{in,fixed} + step$, $V_{in,fixed} - step$ and $V_{in,fixed}$ to save the respective currents. From these new three points, a regression straight line has been created and its intercept has been taken and compared to the previously fixed one. If there is an important variation in its value, the controller can understand if the new optimal V_{in} has increased or decreased. Then when this happens re-start the identification process and find the new optimal working point.

The controller rarely does this process so the frequency is lower with respect to monitoring the input current. This is because most variations can be found by only looking at the input current and this is a very simple and fast method respecting swinging the voltage. The oscillation can also produce some ripple in the output and so maybe a filter needs to be added on the secondary side to guarantee correct behaviour.

4.3   Conclusions

This new control method works as expected in real life environment. When the circuit is properly designed, the converter variations can be controlled by looking at its primary voltage and current behaviour. This is a huge advantage and gives the possibility to avoid the telemetry, control the complete circuit by the primary side and have a very small secondary circuit with only the mandatory components. The control is implemented using a voltage regulator to guarantee a fixed output voltage independently on the coupled factor k and the load value. By using this new architecture approach for a class-E DC-DC converter, it's possible to implement a small circuit in some sensible environments like biomedical ones.

Possible future studies can be devoted to more efficient tracking algorithms or simply to the implementation of a demo, maybe using the proposed solution. The software can be managed to control the laboratory instruments or by a small microcontroller. The power managed by this prototype is 57.6 mW, but in the future, the studies will focus on some converters capable of dealing with higher power levels.

A Python scripts

A1 Input characteristic with different load models

```
###All libraries that need to be imported###

import pandas as pd #database library

import matplotlib.pyplot as plt #graph library

import numpy as np

from numpy import diff #vector library*


# Some example parameters to test constant voltage driven load with a low Gout

Vin=np.linspace(2,100,1000);

gout = 1/500;

Vn = 6;

g = 0.018;

Pn = 4.05;

Gload=Pn/(Vn*Vn)


###Conductance load model###

Vout_cond = (g*Vin)/((Pn/(Vn*Vn))+gout)

Iout_cond = (g*Vin) - (gout*Vout_cond);

Iin_cond = (Vout_cond*Iout_cond)/Vin;

###Norton equivalent load model###

Vout_norton = ((g*Vin)-(Pn/(2*Vn)))/((Pn/(2*(Vn*Vn)))+gout) ;

Iout_norton = (g*Vin) - (gout*Vout_norton);

Iin_norton = (Vout_norton*Iout_norton)/Vin;

###Current generator load model###

Iin_cg=((g*Pn)/(gout*Vn))-(((Pn*Pn)/(gout*Vn*Vn))/Vin);


#Optimal point described but those two equations
```

```
Iin_opt = ((Vn*(g*Vin-gout*Vn))/Vin);

Vin_opt = ((Pn/(g*Vn))+((gout*Vn)/g));


###Final plot###

lab='Iin-Conductance model'

x1=plt.figure(1)

plt.plot(Vin, Iin_cond, label = lab)# plotting the points

plt.xlabel('Vin', color='red')

plt.ylabel('Iin', color='red')

plt.ylim([0,0.15])

lab='Iin-Norton model'

x1=plt.figure(1)

plt.plot(Vin, Iin_norton, label = lab)# plotting the point

lab='Iin-Current generator model'

x1=plt.figure(1)

plt.plot(Vin, Iin_cg, label = lab)# plotting the points

lab='Iin-Shunt on'

x1=plt.figure(1)

plt.plot(Vin, Iin_opt, label = lab)# plotting the points

plt.axis('off')

x1.set_size_inches(9, 7)


# Some example parameters to test constant current driven load with a low Rout

Vin=np.linspace(0.1,10,1000);

Rout = 1/500;

In = 67.5e-3;

alfa = 55;

Pn = 4.05;

Rload=Pn/(In*In)
```

###Resistance load model###

Iout_cond = (alfa*Vin)/((Pn/(In*In))+Rout)

Vout_cond = (alfa*Vin) - (Rout*Iout_cond);

Iin_cond = (Vout_cond*Iout_cond)/Vin;

###Thevenin equivalent load model###

Iout_norton = ((alfa*Vin)-(Pn/(2*In)))/((Pn/(2*(In*In)))+Rout) ;

Vout_norton = (alfa*Vin) - (Rout*Iout_norton)

Iin_norton = (Vout_norton*Iout_norton)/Vin;

###Voltage generator load model###

Iin_cg=((alfa*Pn)/(Rout*In))-(((Pn*Pn)/(Rout*In*In))/Vin);

#Optimal point described but those two equations

Iin_opt = ((In*(alfa*Vin-Rout*In))/Vin);

Vin_opt = ((Pn/(alfa*In))+((Rout*In)/alfa));

###Final plot###

lab='Iin-Resistance model'

x2=plt.figure(2)

plt.plot(Vin, Iin_cond, label = lab)# plotting the points

plt.xlabel('Vin', color='red')

plt.ylabel('Iin', color='red')

plt.ylim([0,5])

plt.xlim([0,2])

lab='Iin-Thevenin model'

x2=plt.figure(2)

plt.plot(Vin, Iin_norton, label = lab)# plotting the points

lab='Iin-Voltage generator model'

x1=plt.figure(2)

plt.plot(Vin, Iin_cg, label = lab)# plotting the points

lab='Iin-Shunt on'

```
x2=plt.figure(2)

plt.plot(Vin, Iin_opt, label = lab)# plotting the points

plt.axis('off')

x2.set_size_inches(9, 7)
```

A2 Intercepts values for different load and distance

```
###All libraries that need to be imported###

import pandas as pd

import numpy as np

from scipy.interpolate import interpn, RegularGridInterpolator

import matplotlib.pyplot as plt

import matplotlib.cm as cmap

import time

from scipy import stats

idx = pd.IndexSlice


###Import values from ones taken from the prototype###

imported_dict = np.load("220607-
Iin_RegularGridInterpolator_ResistiveLoad_FromMeasurements.npy", allow_pickle=True)[()]

iin_interp = imported_dict['interpolator']

vin_vals = imported_dict['vin_vals']

m_vals = imported_dict['m_vals']

rload_vals = imported_dict['rload_vals']
```

Identification with regression method and intercepts – for different M and R_{load}###

```
#Parameters not known a priori

Intercepts=np.zeros(50)

Matrix_inter=np.zeros((50,50))

Iin=np.zeros(50)

#Mobile window
```

```
Iin3=np.zeros(3)

Vin3=np.zeros(3)

Vin0=vin_max

#Flag

f1,f2=0

#Project parameters

#Fixed

step=0.2

#Counters

j=0 # for the M

glob=0

#Cycle

while(f2==0): #all the M

  f1=0

  k=0 #counts Rload

    while(f1==0): #all the Rload

    i=2 #stepper counter

    f=0

     #Iino at Vin_max

    point0 = (vin_max, m_vals[j], rload_vals[k])

    Iin[0]=iin_interp(point0,method='linear')

    # Iin1 at Vin_max-step

    Vin1=vin_max-step

    point1 = (Vin1, m_vals[j], rload_vals[k])

    Iin[1]=iin_interp(point1,method='linear')

    while (f==0):

      Vin1=Vin1-step

      point1 = (Vin1, m_vals[j], rload_vals[k])

      Iin[i]=iin_interp(point1,method='linear')

      #Three Vin
```

```
        Vin3[0]=Vin1+(step*2)

        Vin3[1]=Vin1+step

        Vin3[2]=Vin1

        #Three lin

        lin3[0]=lin[i-2]

        lin3[1]=lin[i-1]

        lin3[2]=lin[i]

        res = stats.linregress(Vin3, lin3)

        Intercepts[i-2]=res.intercept

        i+=1

        #Exit

        if (Vin1<1):

            f=1

            k+=1

    Matrix_inter[glob]=Intercepts

    glob+=1 #charge Matrix_inter

    if (k==5):

        f1=1

        j+=1

  if (j==3):

        f2=1

        j+=1
### Plot of all different intercepts###
x=np.zeros(50)
for i in range (36):
    x[i]=7.46-(i*0.2)
fig, axs = plt.subplots(3,3,figsize=(15,15))
for ax in axs.flat:
    ax.set(xlabel='Vin (V)', ylabel='Intercept value')
cont=0
```

```
for i in range (3):

  j=0

  while (j<3):

    axs[i, j].plot(x, Matrix_inter[cont]*1000,'-')

    axs[i, j].plot(x, Matrix_inter[cont]*1000,'r.')

    b=axs[i, j].set_title(a)

    plt.setp(b, color='r')

    j+=1
```

Bibliography

[1] A. Celentano, F. Pareschi, V. Valente, R. Rovatti, W. A. Serdijn, and G. Setti, "A Wireless Power Transfer System for Biomedical Implants based on an isolated Class-E DC-DC Converter with Power Regulation Capability," in 63rd International Midwest Symposium on Circuits and Systems (MWSCAS). *IEEE*, Aug. 2020, pp. 190–193. doi: 10.1109/MWSCAS48704.2020.9184689.

[2] H. Ueda and H. Koizumi, "Class-e2 DC-DC converter with basic class-e inverter and class-e ZCS rectifier for capacitive power transfer," *IEEE Trans. Circuits Syst.* II Express Briefs, vol. 67, no. 5, pp. 941–945, May 2020. doi: 10.1109/TCSII.2020.2981131.

[3] M. Liu, Y. Qiao, S. Liu, and C. Ma, "Analysis and Design of A Robust Class E2 DC–DC Converter for Megahertz Wireless Power Transfer," *IEEE Trans. Power Electron.*, vol. 32, no. 4, pp. 2835–2845, Apr. 2017. doi: 10.1109/TPEL.2016.2573839.

[4] M.-J. Liu and S. S. H. Hsu, "A Miniature 300-MHz Resonant DC–DC Converter With GaN and CMOS Integrated in IPD Technology," *IEEE Trans. Power Electron.*, vol. 33, no. 11, pp. 9656–9668, Nov. 2018. doi: 10.1109/TPEL.2017.2788946.

[5] I. A. Mashhadi, M. Pahlevani, S. Hor, H. Pahlevani, and E. Adib, "A New Wireless Power-Transfer Circuit for Retinal Prosthesis," *IEEE Trans. Power Electron.*, vol. 34, no. 7, pp. 6425–6439, Jul. 2019. doi: 10.1109/TPEL.2018.2872844.

[6] F. Pareschi, A. Celentano, M. Mangia, R. Rovatti, and G. Setti, "Through-The-Barrier Communications in Isolated Class-E Converters Embedding a Low-K Transformer," in 2020 *IEEE International Symposium on Circuits and Systems (ISCAS)*, Oct. 2020, pp. 1–5. doi: 10.1109/ISCAS45731.2020.9180486.

[7] M. Ghovanloo and S. Atluri, "An integrated full-wave cmos rectifier with built-in back telemetry for rfid and implantable biomedical applications," *IEEE Transactions on Circuits and Systems I: Regular Papers*, vol. 55, no. 10, pp. 3328–3334, Nov. 2008.

[8] M. Kiani and M. Ghovanloo, "An rfid-based closed-loop wireless power transmission system for biomedical applications," *IEEE Transactions on Circuits and Systems II: Express Briefs*, vol. 57, no. 4, pp. 260–264, Apr. 2010.

[9] H. Zhu, B. Zhang, and L. Wu, "Output Power Stabilization for Wireless Power Transfer System Employing Primary-Side-Only Control," *IEEE Access*, vol. 8, pp. 63 735–63 747, 2020. doi: 10.1109/ACCESS.2020.2983465.

[10] V. Valente, C. Eder, A. Demosthenous, and N. Donaldson, "Towards a closed-loop transmitter system with integrated class-D amplifier for coupling-insensitive powering of implants," in 19th *IEEE International Conf. on Electronics*, Circuits, and Systems (ICECS 2012), Dec. 2012, pp. 29–32. doi: 10.1109/ICECS.2012.6463708.

[11] X. Dai, X. Li, Y. Li, and A. P. Hu, "Impedance-Matching Range Extension Method for Maximum Power Transfer Tracking in IPT System," *IEEE Trans. Power Electron.*, vol. 33, no. 5, pp. 4419–4428, May 2018. doi: 10.1109/TPEL.2017.2716968.

[12] P. Perez-Nicoli and F. Silveira, "Maximum Efficiency Point Tracking in Inductive Links: Series Versus Parallel Receiver's Compensation," in 2019 *IEEE Wireless Power Transfer Conference (WPTC)*. London, United Kingdom: IEEE, Jun. 2019, pp. 150–153. doi: 10.1109/WPTC45513.2019.9055556.

[13] Z. Yan, B. Yang, H. Liu, C. Chen, M. Waqas, R. Mai, and Z. He, "Efficiency Improvement of Wireless Power Transfer Based on Multi transmitter System," *IEEE Trans. Power Electron.*, vol. 35, no. 9, pp. 9011–9023, Sep. 2020. doi: 10.1109/TPEL.2020.2971140.

[14] B. Lee, M. Kiani, and M. Ghovanloo, "A Triple-Loop Inductive Power Transmission System for Biomedical Applications," *IEEE Trans. Biomed. Circuits Syst.*, vol. 10, no. 1, pp. 138–148, Feb. 2016. doi: 10.1109/TBCAS.2014.2376965.

[15] N. Bertoni, G. Frattini, R. Massolini, F. Pareschi, R. Rovatti, and G. Setti, "An analytical approach for the design of class-E resonant DC–DC converters," *IEEE Trans. Power Electron.*, vol. 31, no. 11, pp. 7701–7713, Nov. 2016, doi: 10.1109/TPEL.2016.2535387.

[16] F. Pareschi, N. Bertoni, M. Mangia, R. Rovatti, and G. Setti, "A unified design theory for class-E resonant DC–DC converter topologies," *IEEE Access*, vol. 7, pp. 83825–83838, 2019, doi: 10.1109/ACCESS.2019.2922743.

[17] A. Celentano, F. Pareschi, V. Valente, R. Rovatti, W. A. Serdijn and G. Setti, "A Comparison between Class-E DC-DC Design Methodologies for Wireless Power Transfer," *2021 IEEE International Midwest Symposium on Circuits and Systems (MWSCAS)*, 2021, pp. 71-74, doi: 10.1109/MWSCAS47672.2021.9531712.

[18] A. Celentano, F. Pareschi, V. R. Gozalez-Diaz, R. Rovatti and G. Setti, "A Methodology for Practical Design and Optimization of Class-E DC-DC Resonant Converters," in *IEEE Access*, vol. 8, pp. 205568-205589, 2020, doi: 10.1109/ACCESS.2020.3035507.